forests

MDPI

Article

Dimensional Stability and Technological Performance of 13-Year-Old *Simarouba amara* Aubl. Thinning Wood: Pathways to High-Value Product Development

Luiz Paulo Amaringo-Córdova [1,*], Tatiana Mildred Ucañay-Ayllon [1], Jefferson Alexander Rodriguez-Sotelo [2], Hilter Fasabi-Pashanasi [2], Cesar Mori-Montero [3], Oscar Amado Ruiz-Torres [4], Wilson Francisco Guerra-Arévalo [5], Héctor Guerra-Arévalo [6], Uriel Aldava-Pardave [1], Rosario Marilú Bernaola-Paucar [7], Ana Lucía Milagros Vásquez-Vela [8], Edinson Eduardo López-Galán [9], Jhinmy Karc Hemeryth-Bartra [2] and Kevin Isaac Rodriguez-Vasquez [2]

1 Directorate of Research and Technological Development (DIDET), Directorate of Strategic Agricultural Services (DSEA), Pucallpa-Ucayali Agrarian Experimental Station, National Institute for Agrarian Innovation (INIA), Pucallpa 25000, Peru; tucanay@inia.gob.pe (T.M.U.-A.); ualdavapardave@gmail.com (U.A.-P.)
2 Pucallpa Forest Innovation Center (CITEforestal Pucallpa), Production Technology Institute (ITP), Ministry of Production (PRODUCE), Pucallpa 25000, Peru; jrodriguezs@itp.gob.pe (J.A.R.-S.); citeforespuc10@itp.gob.pe (H.F.-P.); jhemeryth@itp.gob.pe (J.K.H.-B.); krodriguez@itp.gob.pe (K.I.R.-V.)
3 Faculty of Forest and Environmental Sciences, National University of Ucayali (UNU), Pucallpa 25000, Peru; cesar_mori@unu.edu.pe
4 Faculty of Systems Engineering and Civil Engineering, National University of Ucayali (UNU), Pucallpa 25000, Peru; oscar_ruiz@unu.edu.pe
5 Doctoral Program in Sciences for Sustainable Development (CIPDES), Toribio Rodríguez de Mendoza National University of Amazonas (UNTRM), Chachapoyas 01001, Peru; wilson.guerra@untrm.edu.pe
6 Directorate of Research on Integrated Forest Management and Ecosystem Services (Bosques), San Martín Regional Directorate IIAP, Peruvian Amazon Research Institute (IIAP), Tarapoto 22002, Peru; hguerra@iiap.gob.pe
7 School of Agroindustrial Engineering, Faculty of Engineering, National Autonomous Altoandina University of Tarma (UNAAT), Junin 12731, Peru; rbernaola@unaat.edu.pe
8 Directorate of Research on Amazonian Societies (Sociodiversity), Peruvian Amazon Research Institute (IIAP), Iquitos-Loreto, Iquitos 16001, Peru; alvasquez@iiap.gob.pe
9 Directorate of Research on Integrated Forest Management and Ecosystem Services (Bosques), Ucayali Regional Directorate IIAP, Peruvian Amazon Research Institute (IIAP), Pucallpa 25000, Peru; elopez@iiap.gob.pe
* Correspondence: lamaringo@inia.gob.pe; Tel.: +51-991213545

Abstract

The valorization of wood derived from thinning operations in tropical plantations represents an alternative to enhance the sustainability and profitability of forest production systems. This study evaluated the hygroscopic, physical, and machining properties of 13-year-old *Simarouba amara* Aubl. thinning wood obtained from a plantation established in the Peruvian Amazon. Two planting spacings (2 × 2 m and 3 × 3 m) and three longitudinal stem positions (base, middle, and apex) were analyzed using a factorial design and generalized linear mixed models. Planting density and longitudinal position significantly influenced ($p < 0.05$) most of the evaluated properties. The saturated moisture content increased from 96.17% at the base to 135.42% at the apex, whereas basic density decreased from 0.45 to 0.30 g cm^{-3}. Volumetric shrinkage ranged from 10.19% to 14.81%, and the dimensional stability index varied between 1.66 and 1.91. The first principal component (PC1) explained 98.4% of the total variance and clearly differentiated the treatments. The wood exhibited excellent performance in planing and molding, good performance in drilling, and fair performance in turning, indicating strong potential for the manufacture of higher value-added products and for sustainable utilization in tropical plantation forests.

Academic Editor: Roberto Zanuttini

Received: 29 June 2026
Revised: 29 July 2026
Accepted: 31 July 2026
Published: 4 August 2026

 https://doi.org/10.3390/f17080915

Keywords: thinning wood; *Simarouba amara* Aubl.; dimensional stability; technological properties; forest plantation

1. Introduction

Thinning wood is a forest by-product derived from silvicultural management practices in forest plantations [1]. Its production is intended to reduce competition for essential resources such as light, water, and nutrients through the selective removal of certain trees [2]. This process enhances diameter growth, vigor, and the overall quality of the remaining individuals within the plantation [3].

Traditionally, this material has been used primarily as a source of energy (firewood or charcoal), resulting in a significant underutilization of a resource that possesses potential for higher value-added products [4]. In this context, the valorization of thinning wood emerges as a key strategy for promoting forest sustainability and the circular economy by utilizing forest residues for industrial applications, thereby reducing pressure on primary forests and improving resource-use efficiency [5].

Simarouba amara Aubl., commonly known as marupá, is a fast-growing tropical forest species valued for its lightweight wood, uniform texture, and relative ease of processing [6]. Its establishment has been promoted in reforestation programs throughout the Amazon region due to its adaptability and economic potential [7–9]. Despite these advantages, scientific information regarding the technological properties of thinning wood from this species remains limited, restricting its incorporation into higher-value and more complex production chains.

The physical properties of wood, including moisture content, density (green, equilibrium, oven-dry, and basic density), shrinkage, and dimensional stability, are essential for determining its suitability for different industrial applications [10]. In particular, dimensional stability, assessed through indicators such as the volumetric shrinkage coefficient and dimensional stability index, plays a crucial role in the manufacture of products requiring precision and durability, including furniture, wood-based panels, and lightweight structural components [11].

In addition, wood machinability, defined as the behavior of wood during machining operations such as planing, molding, drilling, and turning, constitutes a key technological attribute in secondary wood processing [12]. This property is influenced by anatomical characteristics [13], density [14], moisture content [15], and the proportion of juvenile wood [16], directly affecting surface quality, the occurrence of defects (grain tear-out, roughness, and fiber pull-out) [17] and the efficiency of industrial processing operations [18]. The assessment of machinability according to standards such as ASTM D1666-22 [19] allows for the classification of wood suitability for different manufacturing processes and the determination of its potential for products requiring specific levels of finishing quality and dimensional accuracy [20].

Silvicultural management practices, particularly planting density, as well as longitudinal stem position (base, middle, and apex), influence the technological quality of wood by affecting radial growth, cell dimensions, and the proportion of juvenile wood [21,22]. Consequently, these factors have a direct impact on physical properties, dimensional stability, and machinability [23]. Therefore, it is hypothesized that planting density and longitudinal stem position significantly influence the physical properties, dimensional stability, and machinability of *Simarouba amara* Aubl. thinning wood. However, a knowledge gap remains regarding how these factors affect the overall technological performance of thinning wood from this species.

Although several studies have described the physical and mechanical properties of fast-growing tropical woods, including the characterization of *Simarouba amara* with a basic density of approximately 0.40 g·cm^{-3}, a parallel-to-grain compressive strength of 25.25 MPa, and a static bending strength of 27.29 MPa, meeting the technical requirements for furniture manufacturing [6], as well as evaluations of 20–25-year-old Amazonian plantations reporting a basic density of approximately 361 kg·m^{-3} and very low shrinkage [24,25], information on wood obtained from early thinning operations remains limited. Most published studies have focused on mature trees at the final harvest stage or on the isolated characterization of specific wood properties, providing only scarce quantitative evidence on the effects of thinning timing and intensity on basic density, knot characteristics, mechanical properties, and the proportion of juvenile wood [26]. Consequently, the combined effects of initial planting spacing and longitudinal stem position on the hygroscopic behavior, dimensional stability, and workability of thinning wood remain insufficiently documented. Although thinning intensity has been shown to significantly influence green moisture content and shrinkage parameters (tangential, radial, T/R ratio, and volumetric shrinkage) [27], and fast-growing species generally exhibit a high proportion of earlywood, which is more susceptible to moisture-induced movement, checking, and splitting [28], variation in initial moisture content, shrinkage, and other physical properties of thinning wood along the stem under different planting densities has only been investigated in a fragmented manner and for a limited number of model species [29]. This knowledge gap hinders the identification of silvicultural strategies capable of simultaneously optimizing volumetric productivity and wood technological quality, as excessively early or intensive thinning may reduce basic density, increase the proportion of juvenile wood, impair mechanical performance, and ultimately lower the grade of sawn timber [26].

Within this context, the present study evaluates the physical properties, dimensional stability, and machinability of 13-year-old *Simarouba amara* Aubl. thinning wood, considering two planting densities and different longitudinal stem positions. The objective is to determine the influence of these factors on its technological properties, thereby identifying silvicultural conditions that optimize wood performance and promote its utilization in higher value-added products. Ultimately, this contributes to the development of sustainable forest value chains under a circular economy approach.

2. Materials and Methods

2.1. Selection and Origin of Sample Trees

The wood samples were obtained from an experimental plantation of *Simarouba amara* Aubl. established at the Los Mangos Experimental Center, belonging to the Pucallpa Agricultural Experimental Station of the National Institute for Agrarian Innovation (INIA). The plantation is located at kilometer 4.000 of the Federico Basadre Highway, in the district of Calleria, province of Coronel Portillo, Ucayali Department, Peru. The site exhibits the following soil characteristics: pH (4.5–6.1), organic matter content (1.7%–3.0%), textural class (loam), and effective cation exchange capacity (ECEC) ranging from 5.7 to 12.67 cmol(+)/kg [30]. The geographic coordinates of the study area were recorded and delineated as shown in Figure 1. Five trees were selected from each planting density treatment: 2 × 2 m and 3 × 3 m. The selection was based on criteria of uniformity, dominance, health condition, and stem straightness, following the principles established in NTP 251.008, "Wood and Carpentry for Construction. Selection and Collection of Sample" [31] (Figure 2).

https://doi.org/10.3390/f17080915

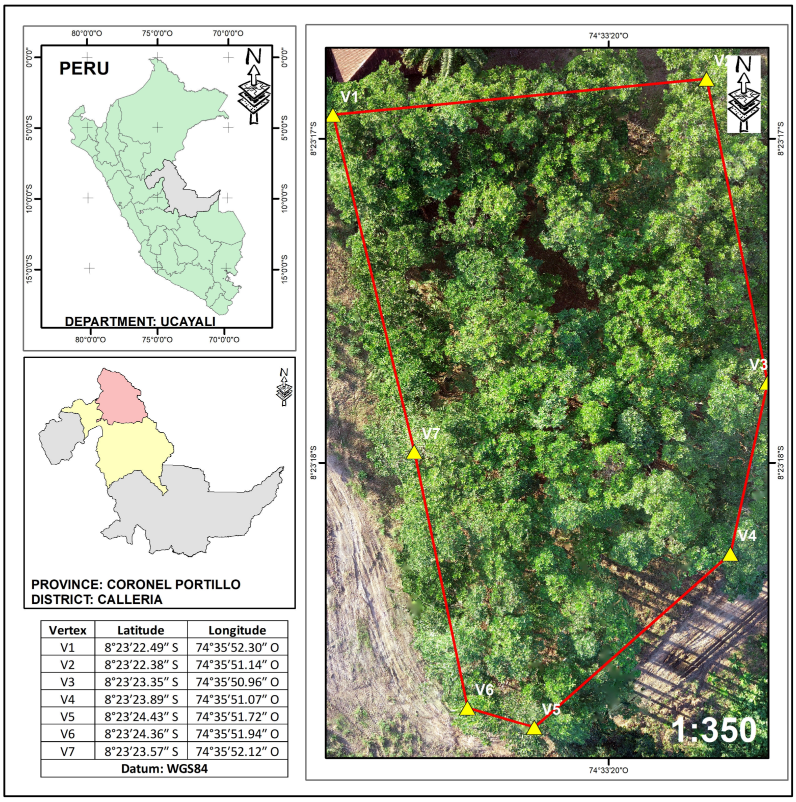

Figure 1. Geographic location of the experimental site (*Simarouba amara* Aubl. plantation) at the Los Mangos Experimental Center, Calleria district, Coronel Portillo province, Ucayali region. The red polygon delineates the study area. Yellow triangles indicate the georeferenced vertices (V1–V7) used to define the plot boundaries. The "+" symbols represent the map coordinate grid.

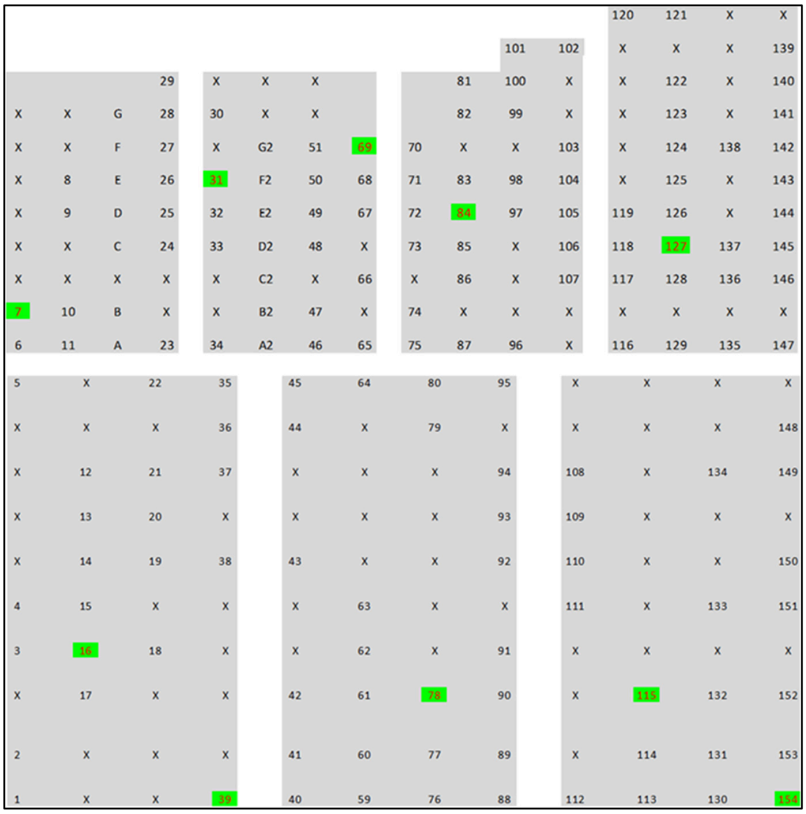

Figure 2. Plantation layout and selection of sample trees for the evaluation of the physical properties of *Simarouba amara* Aubl. thinning wood. The upper panel shows the plantation established at a 2 × 2 m

planting spacing, whereas the lower panel corresponds to the plantation established at a 3 × 3 m planting spacing. The letter "X" indicates trees that were originally planted but did not survive during plantation development. The numbers represent the field identification codes assigned to each tree. The numbers highlighted in green indicate the trees selected for the evaluation of the physical properties of *Simarouba amara* Aubl. thinning wood.

2.2. Dendrometric Characteristics of the Experimental Plantation

The experimental plantation consisted of two adjacent planting-spacing treatments (2 × 2 m and 3 × 3 m), established under the same site conditions and silvicultural management. At the time of sampling, the 2 × 2 m spacing contained 95 trees, whereas the 3 × 3 m spacing contained 66 trees. In the 3 × 3 m spacing, trees exhibited a diameter at breast height (DBH) ranging from 9.80 to 31.19 cm, with a mean DBH of 21.01 cm and a mean total height of 16.16 m. In the 2 × 2 m spacing, DBH ranged from 5.76 to 29.35 cm, with a mean of 18.33 cm, while the mean total tree height was 18.60 m. These dendrometric characteristics indicate that both spacing treatments were developed under comparable environmental conditions, differing primarily in planting spacing and stand density (Table 1).

Table 1. Dendrometric characteristics of the *Simarouba amara* Aubl. plantation.

Planting Spacing	Surviving Trees (No.)	DBH Range (cm)	Mean DBH (cm)	Mean Height (m)
2 × 2 m	95	5.76–29.35	18.33	18.60
3 × 3 m	66	9.80–31.19	21.01	16.16

2.3. Tree Felling and Stem Sectioning

The selected trees were felled using a chainsaw under controlled cutting procedures, following occupational safety protocols and ensuring the preservation of stem integrity. Stem sectioning was performed according to ISO 4471:1982 [32], which establishes procedures for longitudinally dividing the stem into three levels: base (Ba), middle (Me), and apex (Ap). This segmentation allows for the evaluation of wood properties along the axial growth gradient (Figure 3).

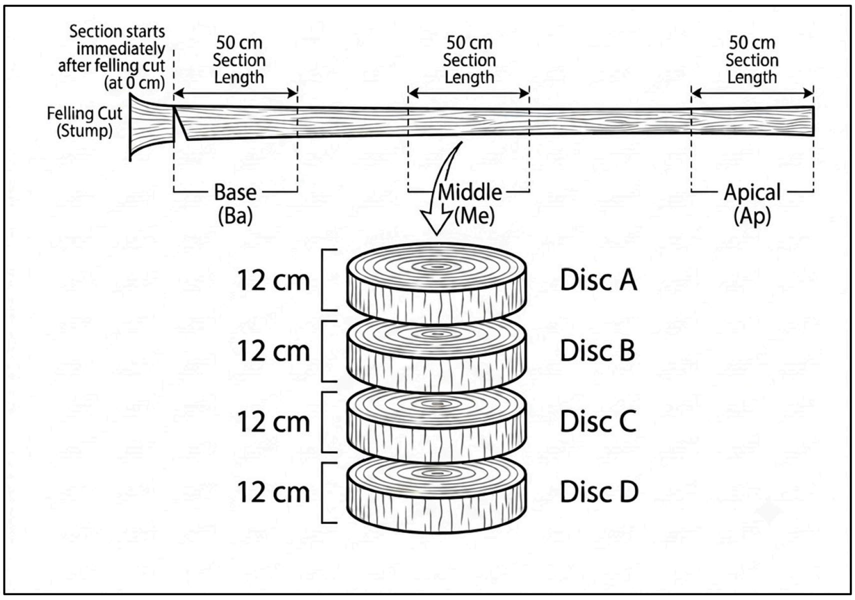

Figure 3. Longitudinal stem sampling scheme and disk preparation of 13-year-old *Simarouba amara* trees.

2.4. Preparation and Coding of Stem Sections

Three 50 cm long stem sections were obtained from the basal (Ba), middle (Me), and apical (Ap) portions of each tree following the sampling procedure described in NTP 251.008 [31]. Subsequently, transverse wood disks were prepared from each stem section for specimen preparation and physical property determination. Immediately after sampling, the stem sections and corresponding wood disks were wrapped in plastic film to minimize moisture loss and labeled with indelible codes to ensure full experimental traceability. The coding system incorporated the following information: species (*Simarouba amara* Aubl.), tree number (1–5), stem position (Ba, Me, Ap), and planting spacing (D1 for 2 × 2 m and D2 for 3 × 3 m), in accordance with NTP 251.008:2016.

2.5. Transportation and Processing of Stem Sections

The stem sections and their corresponding wood disks were transported to the carpentry workshop of the Forest Productive Innovation and Technology Transfer Center of Pucallpa (CITEforestal Pucallpa), where they were processed for specimen preparation. Transportation was carried out under conditions that avoided direct sunlight exposure in order to preserve the initial moisture content of the samples, as recommended by NTP 251.009, "Wood and Carpentry for Construction. Conditioning of Wood Intended for Physical and Mechanical Testing" [33].

2.6. Preparation of Specimens

Based on the previously obtained and coded disks, wood specimens were prepared at the CITEforestal Pucallpa workshop using calibrated machinery to ensure cutting accuracy. Prismatic specimens measuring 3 cm × 3 cm × 10 cm were produced in accordance with Peruvian Technical Standard NTP 251.011 [34]. The specimens were oriented according to the tangential and radial anatomical planes and prepared following the recommendations of ASTM D5536-17 [35]. After specimen preparation, all samples were preconditioned under controlled laboratory conditions (20 °C and 60%–70% relative humidity) prior to testing to minimize uncontrolled moisture variation. Specimens were prepared following the recommendations of ASTM D5536-17. Oven drying at 90 ± 2 °C was carried out exclusively to determine the oven-dry mass required for the calculation of physical properties and was not used as a conditioning treatment before testing.

A total of 691 specimens were obtained. All specimens retained the traceability established during the disk coding process and were organized according to three sampling factors: plantation spacing, longitudinal stem position, and radial location within the cross-sectional area of the log (Figure 4). The samples originated from trees established under two planting spacings (2 m × 2 m, equivalent to 4 m^2 per tree, and 3 m × 3 m, equivalent to 9 m^2 per tree). For each spacing treatment, disks were collected from three longitudinal stem positions (base, middle, and apex) to represent the axial variability of the wood.

From each disk, specimens were obtained from four radial positions (A, B, C, and D), defined as consecutive sectors of the cross-section. Position A corresponded to the initial reference segment of the disk, located near the cutting point; positions B and C represented adjacent sectors toward the interior; position D corresponded to the sector opposite the initial reference point.

This distribution scheme, presented in Table 2, enabled the integration of stem axial variability, radial wood variability, and silvicultural spacing conditions into the sampling design, thereby ensuring an adequate representation of the wood structure under evaluation.

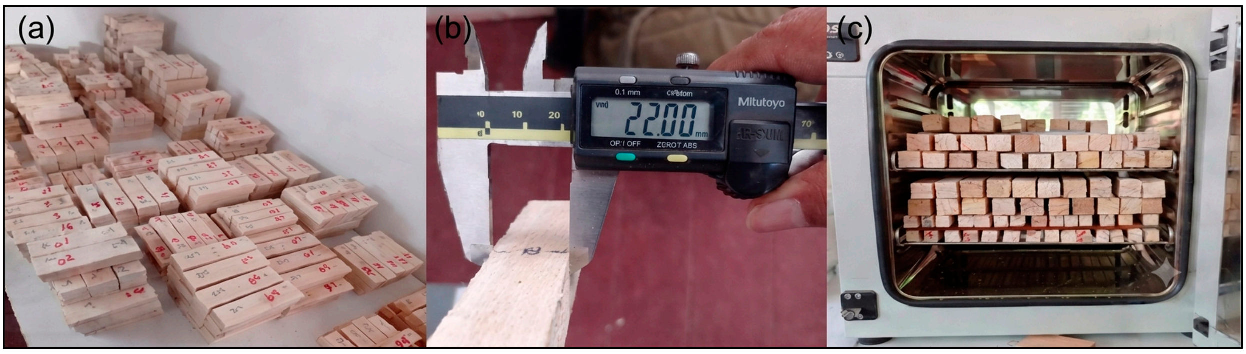

Figure 4. Preparation and conditioning of wood specimens used for the physical and technological characterization of *Simarouba amara* wood. (**a**) Classified and labeled wood specimens prepared from the stem sections; (**b**) dimensional verification of specimen cross-sections using a digital caliper; and (**c**) oven conditioning of the specimens prior to physical property determination.

Table 2. Distribution of evaluated specimens according to planting density, longitudinal stem position, and radial position in thinning wood of *Simarouba amara* Aubl.

Planting Density	Longitudinal Stem Position/Radial Position												Total
	Base				Middle				Apex				
	A	B	C	D	A	B	C	D	A	B	C	D	
$2 \times 2 = 4$ m^2	26	28	26	36	31	36	25	23	30	27	28	30	346
$3 \times 3 = 9$ m^2	33	24	35	23	26	25	29	35	26	33	29	27	345
Subtotal of specimens	59	52	61	59	57	61	54	58	56	60	57	57	691

2.7. Coding of Test Specimens

The test specimens were recoded following the specifications established in NTP 251.008 [31], considering the variables of species, tree number, longitudinal stem position, planting density, and radial position. This coding system allowed for the unambiguous identification of the origin of each sample throughout processing and analysis.

2.8. Experimental Design

The study was conducted under a completely randomized design with a 2×3 factorial arrangement, aimed at analyzing the effect of two factors on the physical properties of thinning wood from *Simarouba amara* Aubl. The first factor corresponded to planting density, evaluated at two spacing levels (2 m $\times$ 2 m and 3 m $\times$ 3 m), while the second factor was represented by longitudinal stem position, with three levels: base, middle, and apex. This design allowed for the evaluation of both the individual effects of each factor and their interaction on the response variables. Both factors were considered fixed effects, as they represent defined experimental conditions of direct interest for comparison. Additionally, the variability associated with radial wood position was incorporated into the model as a random effect through the inclusion of four radial positions (A, B, C, and D) within each disk. This approach allowed the intrinsic variability of the stem to be isolated, improving the precision of the estimated effects.

2.9. Data Analysis

Data processing and statistical analysis were performed using the R programming environment (version 4.5.0), through the RStudio interface. Generalized linear mixed models (GLMMs) were applied using the glmmTMB package, considering different probability distributions, link functions, and, when necessary, the modeling of overdispersion or underdispersion. Model selection for each response variable was based on the lowest Akaike

Information Criterion (AIC). The model specifications, including assumed distribution, link function, and dispersion structure, are detailed in Table 3.

Table 3. Random component, dispersion structure, and model selection criteria.

Variable	Distribution	Link Function	AIC	Dispersion
CHSat	Gamma	Logaritmo	1368	NO
Cheh	Beta	Logit	−4676	NO
PSF	Beta	Logit	−4380	NO
TC	Beta	Logit	−4763	-
RC	Beta	Logit	−5848	-
LC	Beta	Logit	−8060	-
VC	Beta	Logit	−8348	NO
BD	Normal	Logaritmo	−3135	NO
SD	Gamma	Logaritmo	−1978	NO
AD	Tweedi	Logaritmo	−2882	NO
OD	Gamma	Logaritmo	−2968	NO
DSI	Lognormal	Logaritmo	−120	-
VCC	Beta	Logit	−8988	NO

CHSat: saturated moisture content; Cheh: equilibrium moisture content; PSF: fiber saturation point; TC: tangential shrinkage; RC: radial shrinkage; LC: longitudinal shrinkage; VC: volumetric shrinkage; DSI: dimensional stability index; VCC: volumetric shrinkage coefficient; SD: saturated density; AD: air-dry density; OD: oven-dry density; BD: basic density. The "Dispersion" column indicates whether a variable was used to model overdispersion or underdispersion when detected; otherwise, it is reported as NO.

Subsequently, the selected models were validated using the DHARMa package, evaluating assumptions of residual uniformity and absence of outliers, as well as the lack of overdispersion or underdispersion and homogeneity of variances. Once model adequacy was confirmed, marginal means were estimated using the emmeans package, and multiple comparisons among treatments were performed at a significance level of 0.05, applying false discovery rate (FDR) correction. Additionally, univariate generalized linear mixed-effects models (GLMMs) with a beta distribution and logit link were fitted using B-spline basis functions implemented through the *bs*() function to capture potential nonlinear relationships. These models were used to evaluate the relationship between volumetric shrinkage and different wood density measures, as well as the relationship between tangential shrinkage and moisture-related variables (CHSat, Cheh, and PSF). Finally, a principal component analysis was conducted using the factoextra package to identify multivariate association patterns between treatments and the evaluated variables. The validity of the statistical inferences was supported by model diagnostics, selection criteria, and adjusted significance testing procedures.

2.10. Machinability Test

The machinability of thinning wood of *Simarouba amara* Aubl. was evaluated under a quantitative descriptive approach, aimed at assessing the behavior of wood under machining processes representative of the secondary forest industry. The study material was obtained from a 13-year-old plantation established at the Los Mangos Experimental Center of the Pucallpa Agricultural Experimental Station (INIA). Four trees were selected through simple random sampling, considering silvicultural criteria such as stem straightness, good phytosanitary condition, and diameter representativeness. Felling was conducted under controlled harvesting principles, followed by stem sectioning into 1.5 m logs according to ISO 4471 [32].

Log sawing was performed in accordance with NTP 251.008, ensuring the production of specimens with tangential, radial, and oblique cutting planes, which allowed the influence of wood structural anisotropy on machinability behavior to be analyzed [19].

Specimens measuring 2.5 × 10 × 100 cm were prepared for planing, molding, and drilling tests, considering different cutting planes, while specimens measuring 4.5 × 4.5 × 15 cm were prepared for turning tests. Specimen coding allowed for the identification of tree origin and anatomical orientation, ensuring experimental traceability.

Machinability tests included planing, molding, drilling, and turning operations, which were performed under controlled conditions according to the criteria established in NTP 251.008 and ASTM D1666-22. The specimens were conditioned to reach an approximate moisture content of 16%, and all tests considered the influence of grain direction and wood anatomical features on machining performance. In planing, a cutter with a 30° cutting angle and a feed speed of 12 m min^{-1} was used; in molding, a tool with a 25° cutting angle and a rotational speed of 4000 rpm was employed; in drilling, two spindle speeds (320 and 1720 rpm) were evaluated; and in turning, cutting angles of 15° and 45° were applied [36].

Machining quality was determined through the identification and classification of surface defects generated during the operations, including torn grain, raised grain, fuzzy grain, splintering, and surface roughness, following the evaluation criteria established in ASTM D1666-22. For result standardization, the equivalent defect value (VA) equation proposed by [37] was used, allowing qualitative assessment to be transformed into a quantitative indicator. In addition, specific formulas were applied for each test, such as the calculation of knife marks in planing and feed and cutting speed calculations in molding, drilling, and turning, ensuring a comprehensive technical characterization of wood behavior [36].

2.11. Evaluation Variables

The evaluation of physical properties and machinability was carried out at the Wood Technology Laboratory of CITEforestal Pucallpa, located at kilometer 4.2 of the Federico Basadre Highway, Callería District, Coronel Portillo Province, Ucayali Department, Peru. Table 4 presents the evaluated physical properties.

Table 4. Evaluation procedures for technological properties of thinning wood of *Simarouba amara* Aubl.

Variable	Formula	Reference
Saturated moisture content of the specimen (CH)	CH(%) = (Ph − Psh)/Psh × 100	NTP 251.010 [38]
Air-dry moisture content of the specimen (Cheh)	Cheh(%) = (Ph − Pheh)/Pheh × 100	NTP 251.010 [38]
Basic density (BD) (g/cm^3)	BD = Psh/Vh	NTP 251.011 [34]
Saturated density (SD) (g/cm^3)	SD = Ph/Vh	NTP 251.011 [34]
Air-dry density (AD) (g/cm^3)	AD = Psa/Vsa	NTP 251.011 [34]
Oven-dry density (OD) (g/cm^3)	OD = Psh/Vsh	NTP 251.011 [34]
Tangential shrinkage (TC)	TC (%) = (Dht − Dst)/Dht × 100	NTP 251.012 [39]
Radial shrinkage (RC)	RC (%) = (Dhr − Dsr)/Dhr × 100	NTP 251.012 [39]
Longitudinal shrinkage (LC)	LC (%) = (Dhl − Dsl)/Dhl × 100	NTP 251.012 [39]
Volumetric shrinkage (VC)	VC (%) = (Dhv − Dsv)/Dhv × 100	NTP 251.012 [39]
Dimensional stability index: T/R ratio (DSI)	DSI = TC/TR	NTP 251.012 [39]
Volumetric shrinkage coefficient (VCC)	VCC (%) = (V1 − V2)/V2(H1 − H2) × 100	NTP 251.012 [39]
Fiber saturation point (PSF)	PSF (%) = VC/VCC	NTP 251.012 [39]

Ph: wet weight (g); Psh: oven-dry weight (g); Pheh: equilibrium hygroscopic moisture weight (g); Psa: air-dry weight (g); Vh: wet or saturated volume (cm^3); Vsa: air-dry volume (cm^3); Vsh: oven-dry volume (cm^3); Dht, Dhr, Dhl, Dhv: wet dimensions (tangential, radial, longitudinal, volumetric); Dst, Dsr, Dsl, Dsv: oven-dry dimensions (tangential, radial, longitudinal, volumetric); H1, H2: moisture content (%).

Table 5 shows that the evaluation of the "wood machinability" variable was conducted through four dimensions corresponding to machining tests (planing, molding, drilling, and turning). In each case, the defects generated were identified and quantified according to their severity (scale from 1 to 5) and surface extent, in accordance with the criteria of

ASTM D1666-22 [19]. Subsequently, these values were transformed into a quantitative indicator (VA) using the equation proposed by [37], which allowed for standardization of the evaluation and the establishment of the final classification of machinability quality [36].

Table 5. Evaluation of machinability variables in thinning wood of *Simarouba amara* Aubl.

Study Variable	Dimension (Test)	Evaluated Indicators	Measurement Unit/Scale	Instrument/ Technique	Technical Reference
Wood machinability	Planing	Grain tear-out, fuzzy grain, raised grain, knife marks	Defect grade (1–5) and % affected area	Direct observation and recording sheet	D1666-22 [19]
	Molding	Surface roughness, splintered grain, fuzziness	Defect grade (1–5) and % affected area	Direct observation and recording sheet	
	Drilling	Internal roughness, grain rupture, compressed grain	Defect grade (1–5) and % affected area	Direct observation and recording sheet	
	Turning	Splintered grain, fiber tear-out, surface roughness	Defect grade (1–5) and % affected area	Direct observation and recording sheet	
	Global evaluation	Equivalent defect value (VA)	Continuous scale (1.0–5.5)	Mathematical calculation	
	Classification	Machinability quality	Categorical: excellent, good, fair, poor, very poor	Technical interpretation	

2.12. Environmental Conditions During Sampling and Processing

During the stages of extraction, transportation, and specimen preparation, environmental conditions were recorded to minimize their influence on the physical properties of the wood. Field activities were conducted under climatic conditions typical of the lowland Peruvian Amazon, with minimum, maximum, and average temperatures of 21.9 °C, 33.5 °C, and 27.7 °C, respectively. Relative humidity was 70.5%, precipitation was 50.5 mm, sunshine duration was 200.7 h, and wind speed was 2.2 m/s. This information was obtained from the Meteorological Bulletin Vol. 2-2024 of the CP-UNU-Pucallpa Meteorological Station [40] during the sampling period in August 2024.

Subsequently, in the Wood Technology Laboratory of CITEforestal Pucallpa, stable environmental conditions were maintained with a temperature of 20 °C and average relative humidity between 60% and 70%, allowing all specimens to be preconditioned under identical environmental conditions prior to oven drying, thereby minimizing uncontrolled moisture variation among samples. Critical handling stages were performed in minimal time to reduce uncontrolled moisture loss. These conditions are considered relevant due to their influence on density, shrinkage, and moisture content, which are key parameters evaluated in this study and must be measured under controlled or properly recorded environmental conditions to ensure result reliability (NTP 251.011).

Soil physicochemical analysis revealed a forest ecosystem characterized by acidic conditions ranging from moderately acidic (pH 5.8–6.1) to strongly acidic (pH 4.5). Organic matter content varied from low to medium (1.70% to 3.00%), while effective cation exchange capacity (ECEC) remained at low to moderate levels (5.70 to 14.73 cmol(+) kg^{-1}). Physically, the soil presented a predominantly loamy texture, with localized variations toward clay loam and sandy loam classes [30]. The recording of these edaphoclimatic parameters suggests that, despite natural soil variability, site conditions maintained relative environmental uniformity.

3. Results

3.1. Hygroscopic Properties of Thinning Wood of Simarouba amara Aubl.

The ANOVA results indicated that the hygroscopic properties of *Simarouba amara* Aubl. thinning wood were significantly influenced by both the longitudinal stem level (NLF) and planting density (DS) ($p < 0.01$). A significant interaction effect (NLFxDS) was also observed for CHSat, Cheh, and PSF. In contrast, the effect of radial position was practically null. The models showed a high explanatory capacity, with marginal R^2 values ranging from 0.69 to 1.00.

In agreement with these results, Figure 5 shows multiple comparisons where significant differences in the NLFxDS interaction were observed for CHSat, PSF, and Cheh, exhibiting consistent patterns along the stem. For CHSat, a progressive and clearly differentiated increase from the base to the apex was observed in both DS levels. Under the 2 × 2 m spacing, values increased from 96.17% at the base to 109.09% in the middle section and 125.38% at the apex. The same trend was observed in the 3 × 3 m spacing, although with higher values at each level: 106.94% at the base and 122.06% in the middle section, reaching a maximum of 135.42% at the apex. Differences between DS were evident at all longitudinal levels, being more pronounced at the apical section, where the greatest separation between treatments was recorded.

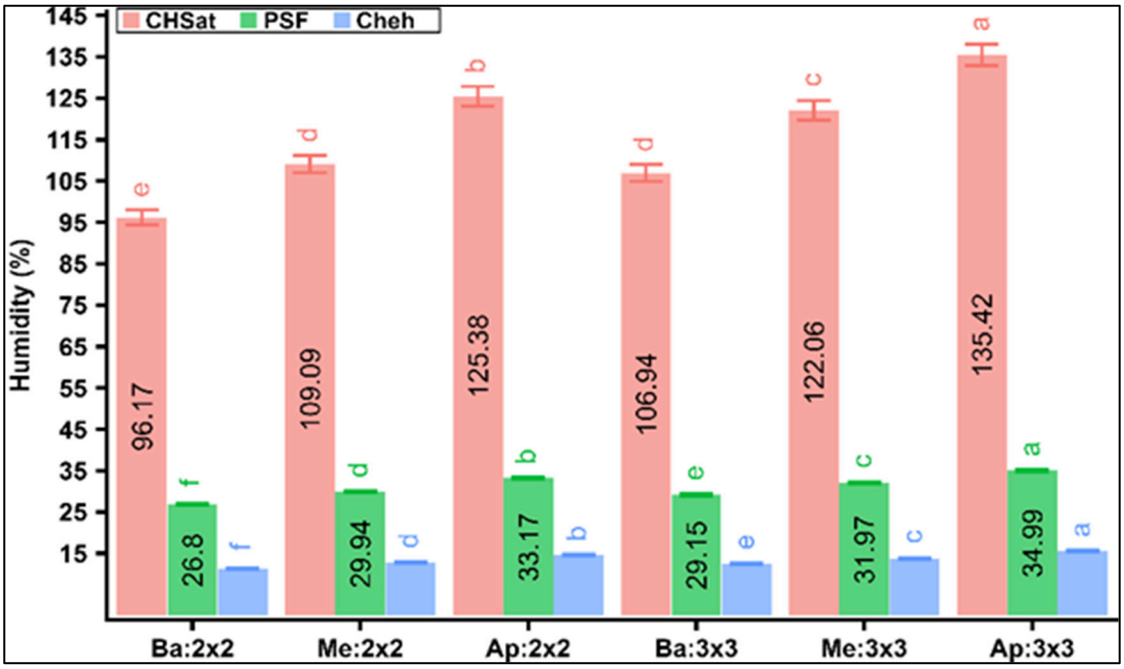

Figure 5. Variation in the hygroscopic properties of thinning wood of *Simarouba amara* Aubl. according to longitudinal stem position and planting density. CHSat: Saturated Moisture Content; Cheh: Equilibrium Moisture Content; PSF: Fiber Saturation Point; Ba: 2 × 2: base of the stem with 4 m^2 spacing; Me: 2 × 2: middle of the stem with 4 m^2 spacing; Ap: 2 × 2: apex of the stem with 4 m^2 spacing; Ba: 3 × 3: base of the stem with 9 m^2 spacing; Me: 3 × 3: middle of the stem with 9 m^2 spacing; Ap: 3 × 3: apex of the stem with 9 m^2 spacing. Means that do not share a common letter are significantly different ($p < 0.05$).

For PSF, a similar pattern of increase from the base toward the apex was observed, with significant differences between longitudinal levels within each planting density. Under the 2 × 2 m spacing, values were 26.8% at the base, 29.94% in the middle section, and

33.17% at the apex. Under the 3 × 3 m spacing, the corresponding values were 29.15%, 31.97%, and 34.99%, respectively, with this last value being the highest observed. As with CHSat, at all longitudinal levels the 3 × 3 m spacing showed higher values than the 2 × 2 m spacing, maintaining a consistent trend of differentiation between spacings. Regarding Cheh, although differences were less pronounced compared to the other variables, a gradual increase from the base toward the apex was also observed in both densities. Under the 2 × 2 m spacing, mean values were 11.42% at the base, 12.84% in the middle section, and 14.57% at the apex. Under the 3 × 3 m spacing, the corresponding values were approximately 12.5% at the base, 13.79% in the middle section, and 15.54% at the apex. In this case, although differences between densities were smaller, the pattern of higher values under the 3 × 3 m spacing was maintained throughout the stem. Overall, the results shown in Figure 5 evidence a clear differentiation both by longitudinal stem level and planting density, with consistent increases from base to apex and systematically higher values under the 3 × 3 m spacing for the three hygroscopic properties evaluated.

3.2. Density of Thinning Wood of Simarouba amara Aubl.

Wood densities of *Simarouba amara* Aubl. thinning wood were significantly affected by longitudinal stem level (NLF) and planting density (DS) ($p < 0.01$) for all evaluated properties: basic density (BD), saturated density (SD), air-dry density (AD), and oven-dry density (OD). The NLFxDS interaction was not significant for BD, SD, and OD ($p > 0.05$), whereas a significant interaction was observed for AD ($p = 0.04$), indicating a differentiated response depending on the combination of both factors. Additionally, the effect of radial position was minimal, and the models showed good fit, with marginal R^2 values ranging from 0.59 to 0.97.

According to Figure 6, saturated density (SD) showed its highest values at the base of the stem and a progressive decrease toward the apex. Under the 2 × 2 m spacing, values were 1.09 g cm^{-3} at the base, 1.01 g cm^{-3} in the middle section, and 0.92 g cm^{-3} at the apex. For the 3 × 3 m spacing, the corresponding values were 1.02, 0.95, and 0.88 g cm^{-3}. At all longitudinal levels, the 2 × 2 m spacing exhibited higher values than the 3 × 3 m spacing. For air-dry density (AD), a decreasing trend along the stem was also observed in both planting densities. Under the 2 × 2 m condition, values were 0.52 g cm^{-3} at the base, 0.46 g cm^{-3} in the middle section, and 0.40 g cm^{-3} at the apex. Under the 3 × 3 m spacing, the corresponding values were 0.47, 0.43, and 0.36 g cm^{-3}. This variable also showed a significant interaction, reflected in more marked differences among treatment combinations.

Regarding OD, the values also decreased from the base toward the apex. Under the 2 × 2 m spacing, values of 0.49, 0.42, and 0.36 g cm^{-3} were recorded for the base, middle section, and apex, respectively, while under 3 × 3 m, the values were 0.43, 0.38, and 0.32 g cm^{-3}. In all cases, higher values were observed under the higher planting density. Finally, basic density (BD) presented the lowest values among the evaluated variables, showing a similar decreasing pattern along the stem. Under the 2 × 2 m spacing, values were 0.45 g cm^{-3} at the base, 0.40 g cm^{-3} in the middle section, and 0.34 g cm^{-3} at the apex, while under the 3 × 3 m spacing, values were 0.41, 0.36, and 0.30 g cm^{-3}, respectively. Overall, Figure 5 shows a consistent decrease in wood density from the base toward the apex, as well as systematically higher values under the 2 × 2 m spacing for all evaluated variables.

https://doi.org/10.3390/f17080915

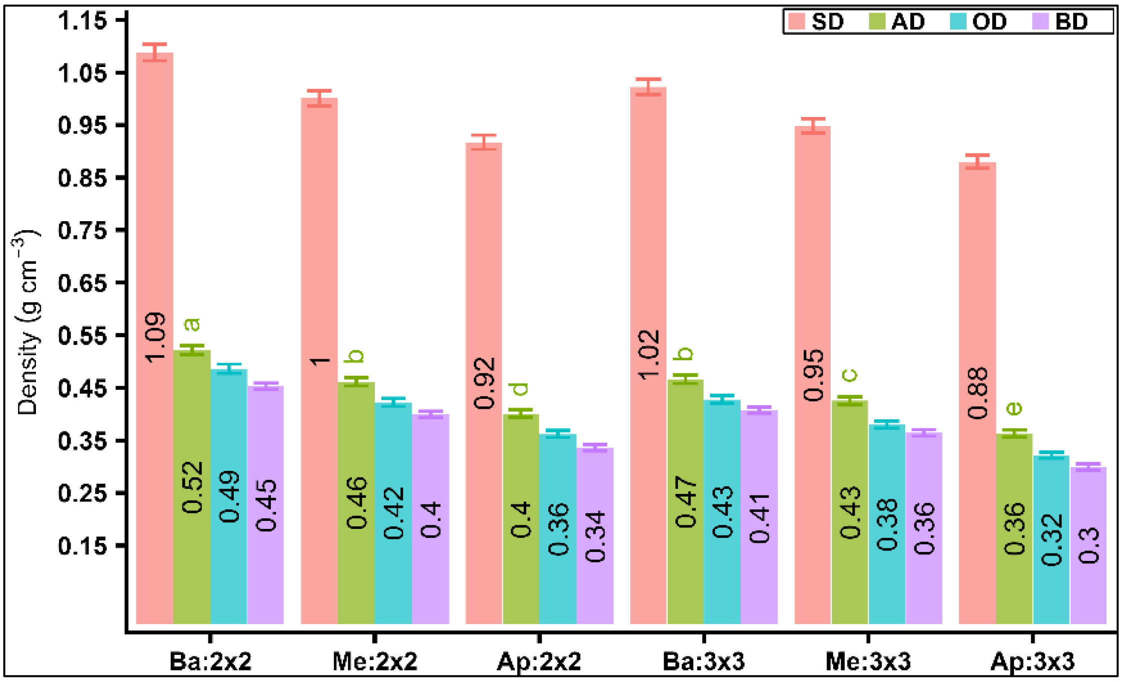

Figure 6. Variation in wood density of thinning wood of *Simarouba amara* Aubl. according to longitudinal stem position and planting density. SD: Saturated Density; AD: Air-dry Density; OD: Oven-dry Density; BD: Basic Density; Ba: 2 × 2: base of the stem with 4 m^2 spacing; Me: 2 × 2: middle of the stem with 4 m^2 spacing; Ap: 2 × 2: apex of the stem with 4 m^2 spacing; Ba: 3 × 3: base of the stem with 9 m^2 spacing; Me: 3 × 3: middle of the stem with 9 m^2 spacing; Ap: 3 × 3: apex of the stem with 9 m^2 spacing. Means that do not share a common letter are significantly different ($p < 0.05$).

3.3. Shrinkage of Thinning Wood of Simarouba amara Aubl.

Wood shrinkage of *Simarouba amara* Aubl. thinning wood was significantly influenced by longitudinal stem position (NLF) and planting density (DS) ($p < 0.01$) for all evaluated variables: tangential shrinkage (TC), radial shrinkage (RC), longitudinal shrinkage (LC), and volumetric shrinkage (VC). Likewise, the NLFxDS interaction showed significant effects for all shrinkage variables ($p \leq 0.01$), indicating that the response of these properties depends on the combination of both factors. Figure 7 shows that volumetric shrinkage (VC) presents a well-defined gradient along the stem, with progressive increases from the base toward the apex in both spacing treatments. Under the 2 × 2 m spacing, values ranged from 10.19% at the base to 12.05% in the middle section and 13.80% at the apex. Under the 3 × 3 m spacing, this trend was more pronounced, reaching 11.56%, 13.27%, and 14.81%, respectively. It is particularly noteworthy that the difference between planting densities increases along the stem, being more evident in the middle section and especially at the apex.

For tangential shrinkage (TC), a behavior consistent with that described for VC was observed, although with less pronounced variation. Under the 2 × 2 m spacing, values increased from 6.22% at the base to 7.41% in the middle section and 8.82% at the apex. Under the 3 × 3 m spacing, these values increased to 6.98%, 8.28%, and 9.40%, respectively. The separation between spacings was consistent across all stem levels, maintaining a relatively stable difference, although slightly greater at the upper section of the stem.

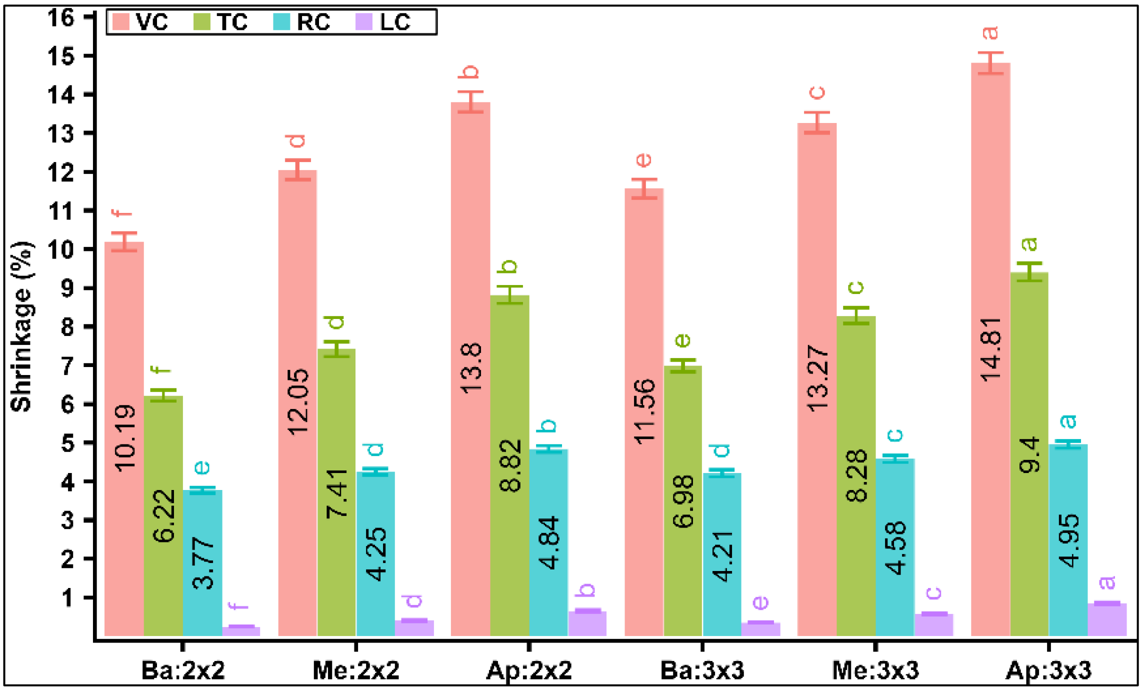

Figure 7. Variation in shrinkage properties of thinning wood of *Simarouba amara* Aubl. according to longitudinal stem position and planting density. TC: Tangential Shrinkage; RC: Radial Shrinkage; LC: Longitudinal Shrinkage; VC: Volumetric Shrinkage; Ba: 2 × 2: base of the stem with 4 m^2 spacing; Me: 2 × 2: middle of the stem with 4 m^2 spacing; Ap: 2 × 2: apex of the stem with 4 m^2 spacing; Ba: 3 × 3: base of the stem with 9 m^2 spacing; Me: 3 × 3: middle of the stem with 9 m^2 spacing; Ap: 3 × 3: apex of the stem with 9 m^2 spacing. Means that do not share a common letter are significantly different ($p < 0.05$).

Radial shrinkage (RC) and longitudinal shrinkage (LC) exhibited narrower ranges of variation. RC ranged from 3.77% to 4.95%, while LC remained below 1% (0.25%–0.85%). However, both variables maintained an increasing trend from the base toward the apex and higher values under the 3 × 3 m spacing. These results indicate that longitudinal stem position (NLF) and planting density (DS) generate differentiated shrinkage patterns, being more pronounced in VC and TC, where differences between treatments become more evident toward the upper stem sections.

3.4. Other Properties of Thinning Wood of Simarouba amara Aubl.

The dimensional stability index (DSI) and volumetric shrinkage coefficient (VCC) of *Simarouba amara* Aubl. thinning wood were significantly affected by longitudinal stem position (NLF) and planting density (DS) ($p < 0.01$). However, the NLF × DS interaction was not significant for any of the evaluated variables ($p > 0.05$), suggesting that both factors act independently on these properties. Likewise, the effect of radial position was negligible, and the model showed high explanatory power for VCC, with a marginal R^2 of 0.97.

In Figure 8, the dimensional stability index (DSI) shows a narrow range of variation among treatments, with values between 1.66 and 1.91. The highest value was recorded at the apex under 3 × 3 m spacing (1.91), followed by slightly lower values at the apex under 2 × 2 m spacing (1.84) and at the middle section under 3 × 3 m spacing (1.82). At the middle section under 2 × 2 m spacing, the value was 1.76, while the lowest values were observed at the base, with 1.67 under 3 × 3 m spacing and 1.66 under 2 × 2 m spacing. The distribution indicates a slight decrease from apex to base, as well as moderate differences between planting densities.

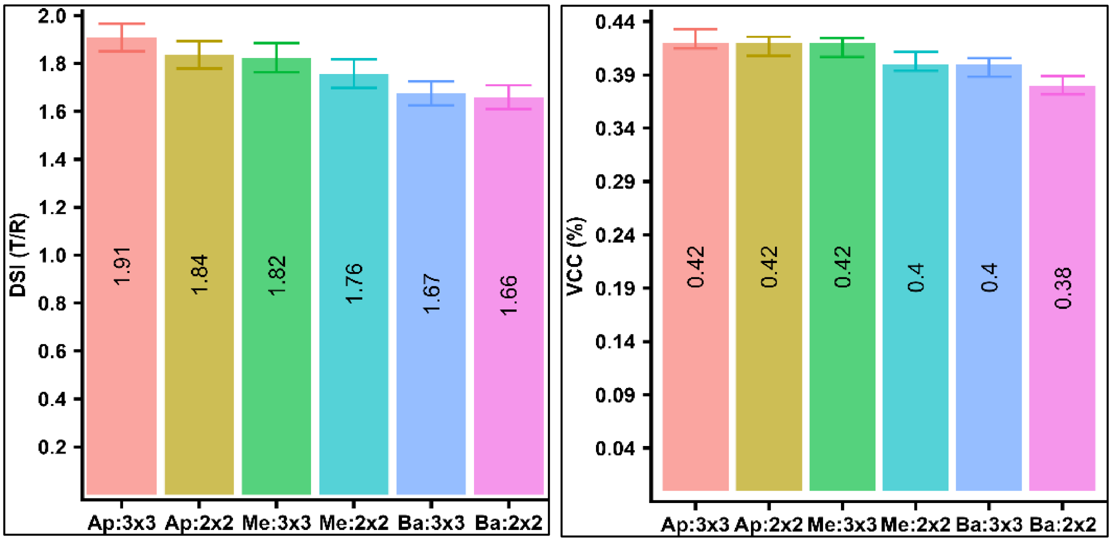

Figure 8. Variation of the dimensional stability index and volumetric shrinkage coefficient of thinning wood of *Simarouba amara* Aubl. according to longitudinal stem position and planting density. DSI: Dimensional Stability Index; VCC: Volumetric Shrinkage Coefficient; Ba: 2 × 2: base of the stem with 4 m^2 spacing; Me: 2 × 2: middle of the stem with 4 m^2 spacing; Ap: 2 × 2: apex of the stem with 4 m^2 spacing; Ba: 3 × 3: base of the stem with 9 m^2 spacing; Me: 3 × 3: middle of the stem with 9 m^2 spacing; Ap: 3 × 3: apex of the stem with 9 m^2 spacing.

Regarding VCC, a narrower range of variation was observed, with values between 0.38 and 0.42. The highest values (0.42) were recorded at the apex under both spacings (2 × 2 m and 3 × 3 m), as well as at the middle section under 3 × 3 m spacing. At the middle section under 2 × 2 m and the base under 3 × 3 m spacing, values were 0.40, while the lowest value (0.38) was observed at the base under 2 × 2 m spacing. Overall, the results show a relatively homogeneous distribution among treatments, with slight variations associated with stem position. In general, Figure 8 reflects that both DSI and VCC exhibit lower variability compared to previously analyzed properties, while still maintaining detectable differences mainly associated with longitudinal stem position.

3.5. Relationship Between Density and Volumetric Shrinkage of Thinning Wood from Simarouba amara Aubl.

The association between wood densities (basic, saturated, air-dry, and oven-dry) and volumetric shrinkage allows for the identification of physical behavior patterns in thinning wood, which is particularly relevant for predicting dimensional stability and performance in processing and end use applications. In this context, univariate GLMM regression models with beta distribution and logit link function were fitted to evaluate the relationship between volumetric shrinkage and the different types of wood density.

In Figure 9, the curves corresponding to basic density (BD), air-dry density (AD), and oven-dry density (OD) show a highly consistent behavior, characterized by a positive and progressive relationship with volumetric shrinkage (VC). In all three cases, VC increases from values close to 10%–11% at low density ranges to approximately 14%–15% at higher density levels, maintaining very similar trajectories throughout the evaluated interval. This functional overlap indicates that these variables have a comparable capacity to describe the variation in volumetric shrinkage. Additionally, the slightly convex shape of the curves reflects an increase in VC sensitivity at higher density ranges, where small changes result in more pronounced increases in shrinkage.

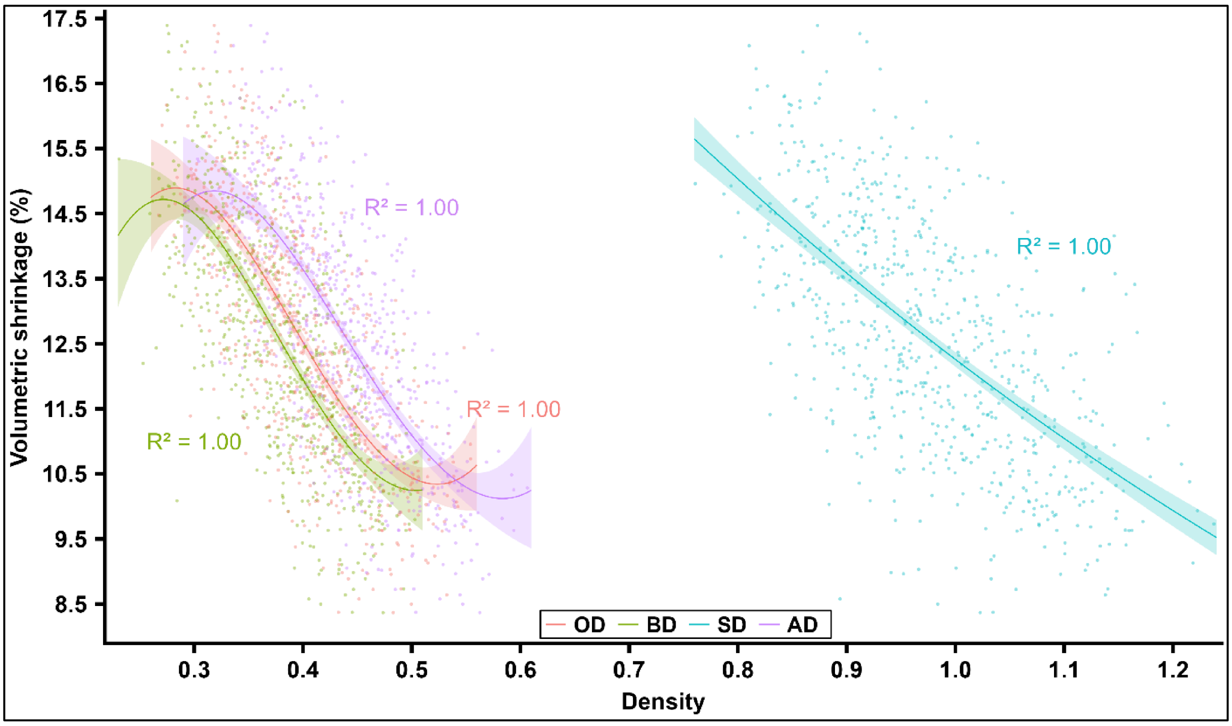

Figure 9. Beta regression models between volumetric shrinkage and different wood density measures of thinning wood from *Simarouba amara* Aubl. Colored dots represent observed data points, solid lines represent fitted Beta regression curves, and shaded areas represent 95% confidence intervals. SD: Saturated Density; AD: Air-dry Density; OD: Oven-dry Density; BD: Basic Density.

In contrast, saturated density (SD) shows a clearly differentiated trajectory, with a steeper slope and a progressive separation from the other variables, particularly in the medium- and high-density ranges. Although the VC variation range remains between 10% and 15%, the greater inclination of the curve indicates a more sensitive response of shrinkage to changes in this variable. This behavior suggests that SD captures more strongly the variations associated with dimensional changes in wood, positioning itself as a more reactive indicator within the analyzed set. Overall, while BD, AD, and OD define a homogeneous behavioral core, SD introduces an additional level of differentiation in the relationship, evidencing that not all density types contribute equally to explaining the variability in volumetric shrinkage.

3.6. Relationship Between Moisture Content and Tangential Shrinkage of Thinning Wood of Simarouba amara Aubl.

The association between moisture content variables (CHSat, Cheh, and PSF) and tangential shrinkage allows for visualization of the relationship between the hygroscopic state of wood and its dimensional behavior. For this purpose, univariate GLMM regression models with beta distribution and logit link function were fitted to evaluate the response of tangential shrinkage as a function of each moisture content variable.

This relationship shows a consistent pattern of increasing shrinkage as moisture levels increase (Figure 10). For equilibrium moisture content (Cheh), tangential shrinkage values range approximately between 6% and 10%, showing a well-defined increasing trend within a narrow moisture range (12%–16%). The fitted curve presents a sustained positive slope, with slight stabilization at higher values, suggesting a progressive but moderate response within this interval.

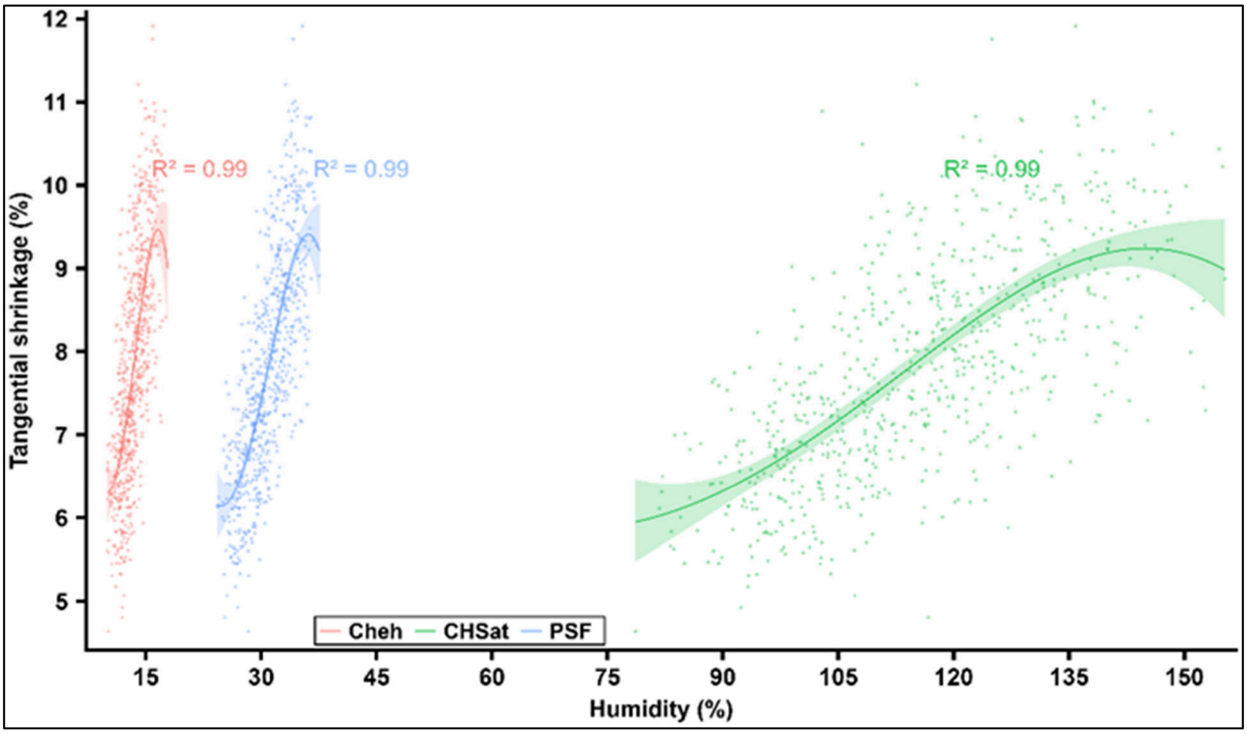

Figure 10. Beta regression models between tangential shrinkage and moisture content variables of thinning wood from *Simarouba amara* Aubl. Colored dots represent observed data points, solid lines represent fitted Beta regression curves, and shaded areas represent 95% confidence intervals. CHSat: Saturated Moisture Content; Cheh: Equilibrium Moisture Content; PSF: Fiber Saturation Point.

In the case of fiber saturation point (PSF), the relationship maintains a similar increasing trend, although shifted toward higher moisture values (28%–35%). Tangential shrinkage varies approximately between 6% and 10%, with a steeper slope compared to Cheh, particularly in the midsection of the curve. Data dispersion is slightly higher, although alignment with the fitted curve remains consistent, evidencing a structured behavior.

For saturated moisture content (CHSat), the widest variation range is observed (80%–150%), where tangential shrinkage increases from values close to 6% up to approximately 9%–9.5%. The curve shows a nonlinear behavior, with a positive slope in the low and medium ranges, followed by a tendency toward stabilization and even a slight decrease at the highest moisture values. This change in slope suggests a transition in wood response beyond certain moisture levels.

The coefficient of determination (R^2 = 0.99 in all cases) indicates a highly robust model fit, reflecting a strong association between tangential shrinkage and the evaluated moisture content variables. Overall, the results demonstrate a well-defined positive relationship, with differences in curve shape and slope intensity depending on the hygroscopic variable, allowing for the identification of specific behaviors within the same phenomenon.

3.7. Principal Component Analysis

Principal component analysis (PCA) was applied to integrate and synthesize the information contained in the set of evaluated physical variables, allowing for a joint exploration of the relationships among hygroscopic properties, densities, and shrinkage of thinning wood from *Simarouba amara* Aubl. This multivariate approach facilitates the identification of association patterns, variation gradients, and potential groupings among treatments, providing a simplified representation of the data structure without losing the essential variability of the system.

Figure 11 presents the PCA results, where the first two axes explain the largest proportion of total variability, with 98.40% for the first principal component (PC1) and 0.60% for the second principal component (PC2). The distribution of treatments along PC1 shows a clear differentiation, making this axis the main gradient of variation. In this sense, treatments corresponding to the apex at 3 × 3 m spacing (Ap: 3 × 3) are located at the positive extreme of PC1, while the base at 2 × 2 m (Ba: 2 × 2) is positioned at the negative extreme, showing a marked separation between contrasting structural conditions. The remaining treatments are distributed in intermediate positions, following a progressive order associated with both longitudinal stem position and planting density.

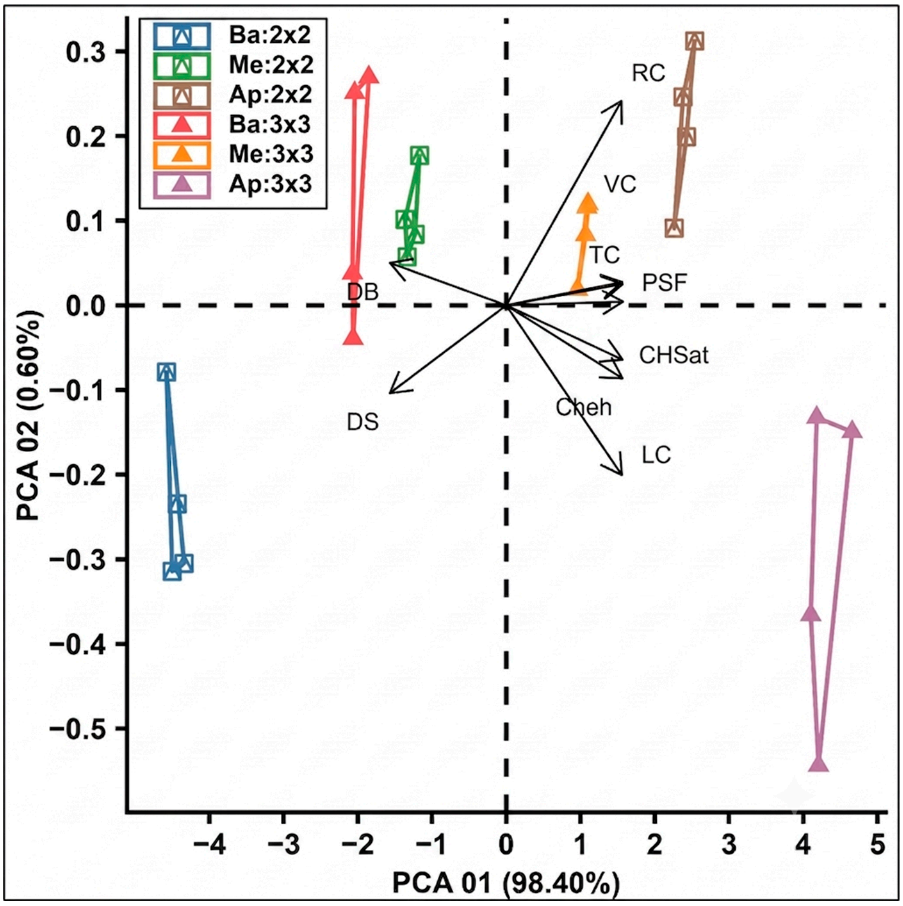

Figure 11. Principal component analysis (PCA) of the physical properties of thinning wood of *Simarouba amara* Aubl. according to longitudinal stem position and planting density. CHSat: Saturated Moisture Content; Cheh: Equilibrium Moisture Content; PSF: Fiber Saturation Point; SD: Saturated Density; AD: Air-dry Density; OD: Oven-dry Density; BD: Basic Density; TC: Tangential Shrinkage; RC: Radial Shrinkage; LC: Longitudinal Shrinkage; VC: Volumetric Shrinkage; DSI: Dimensional Stability Index; VCC: Volumetric Shrinkage Coefficient; Ba: 2 × 2: stem base with 4 m^2 spacing; Me: 2 × 2: middle stem section with 4 m^2 spacing; Ap: 2 × 2: stem apex with 4 m^2 spacing; Ba: 3 × 3: stem base with 9 m^2 spacing; Me: 3 × 3: middle stem section with 9 m^2 spacing; Ap: 3 × 3: stem apex with 9 m^2 spacing.

The orientation of the vectors indicates that variables such as the volumetric shrinkage (VC), radial shrinkage (RC), tangential shrinkage (TC) and the fiber saturation point (PSF) present positive loadings on PC1, aligning in the same direction as the treatments located on the right side of the plot. Similarly, the saturated moisture content (CHSat) and the equilibrium moisture content (Cheh) also show a positive association with this axis, although with lower relative magnitude. In contrast, the basic density (DB) and the dry density (DS) are oriented toward the negative side of PC1, indicating an opposite relationship with the aforementioned variables.

On the vertical axis (PC2), variability is considerably lower; however, it allows certain nuances in the distribution of treatments to be distinguished. For example, the treatments at the stem apex in 2 × 2 (Ap: 2 × 2) and in 3 × 3 (Ap: 3 × 3) present positive values on this axis, whereas Ba: 2 × 2 and Ap: 3 × 3 show greater dispersion toward negative values, evidencing internal variability within these groups. Likewise, the direction of variables such as RC and TC toward positive values of PC2 suggests a slight differentiation with respect to variables such as Cheh and LC, which are oriented toward negative values.

The overall configuration of the biplot shows well-defined groupings of treatments. Those corresponding to the base at 2 × 2 (Ba: 2 × 2) are clearly isolated at the negative extreme of PC1, while those at the apex in 3 × 3 (Ap: 3 × 3) cluster at the opposite extreme, showing a well-defined structural separation. Intermediate treatments, such as Me: 2 × 2 and Me: 3 × 3, are located in central positions, reflecting transitional conditions between both extremes. This arrangement suggests a continuous gradient in the evaluated properties, where longitudinal position and planting density jointly influence the multivariate configuration of the thinning wood from *Simarouba amara* Aubl.

Therefore, the PCA proposes a clear structuring of the treatments, dominated by principal component 1, where the variables associated with shrinkage and moisture content cluster toward positive values, while the density variables are oriented in the opposite direction, allowing for a consistent differentiation of the combined effects of the evaluated factors.

3.8. Machinability

Table 6 shows the results of the machinability evaluation of *Simarouba amara* Aubl. wood, obtained from thinning operations in a thirteen-year-old plantation in the Ucayali region. The results evidence differentiated behavior according to the machining test, based on the equivalent defect values (VA) obtained and their corresponding classification under ASTM D1666-22. In the planing test, the wood presented an average VA value of 1.18, placing it within the "Excellent" quality range. This result indicates a surface largely free of defects, with minimal presence of grain tear-out or fuzziness, suggesting an adequate response to longitudinal cutting, even considering variations in grain orientation.

Table 6. Machinability evaluation of thinning wood of *Simarouba amara* Aubl.

Test	Number of Specimens	Predominant Evaluated Defects	Mean VA	Quality Range (VA)	ASTM D1666-22 Classification
Planing	60	Grain tear-out, fuzziness, raised grain, knife marks	1.18	1.0–1.5	Excellent
Molding	60	Roughness, splintered grain, fuzziness	1.02	1.0–1.5	Excellent
Drilling	60	Internal roughness, grain rupture, compressed grain	1.88	1.6–2.5	Good
Turning	30	Splintered grain, surface roughness, fiber tearing	2.68	2.6–3.5	Fair

In the molding test, an average VA value of 1.02 was obtained, also classified as "Excellent", representing the best performance among the evaluated machining processes. The low incidence of defects such as surface roughness and splintered grain indicates that the wood presents optimal conditions for profiling operations, maintaining dimensional stability and a uniform surface quality. This behavior suggests a high suitability of the species for applications requiring fine finishes and precision machining.

For the drilling test, an average VA value of 1.88 was recorded, corresponding to a "Good" classification. In this case, moderate defects were observed, mainly associated with internal roughness and slight grain compression, indicating that although the wood responds favorably to the process, limitations may arise in operations involving drilling, especially under higher spindle speed conditions. Nevertheless, these defects can be corrected through subsequent finishing processes, maintaining its viability for industrial applications.

Finally, the turning test showed the least favorable performance, with an average VA value of 2.68, classified as "Fair". This result reflects a higher incidence of defects such as fiber tearing, splintered grain, and surface roughness, mainly associated with the interaction between the anatomical structure of the wood and cutting conditions. The observed variability suggests that turning performance is more sensitive to operational factors such as tool angle and process stability, which partially limits its use in high-quality turned products. Overall, the results demonstrate that the machining performance of *Simarouba amara* varied according to the machining operation rather than exhibiting a uniform response across all evaluated processes. Operations involving continuous cutting parallel to the grain consistently produced superior surface quality, whereas turning was more susceptible to defects associated with wood anatomical characteristics and machining conditions. These findings highlight the technological potential of this species for manufacturing value-added wood products requiring high surface quality during secondary wood processing.

3.9. Prototype Development from Thinning Wood of Simarouba amara Aubl.

Based on the results obtained from the machinability evaluation and considering the previously described physical behavior of thinning wood from *Simarouba amara* Aubl., functional prototypes consisting of solid wood doors and desks were developed, with the purpose of validating its performance under real use and processing conditions. These prototypes enabled the integration of experimental results into an applied context, evidencing the material's response during dimensioning, assembly, and surface finishing processes. A total volume of 3.569 m^3 of sawn and kiln-dried thinning wood was used for the development of the prototypes, from which two desks and two solid wood doors were manufactured. The production process of these prototypes is shown in Figure 12. Of this volume, approximately 0.21 m^3 corresponded to the desk prototypes and 0.17 m^3 to the door prototypes, considering losses associated with dimensioning, squaring, and finishing operations. The design and construction characteristics of these prototypes are presented as complementary information, where the dimensional and configurational aspects of each developed product are detailed.

In the case of the solid wood doors, the manufacturing process showed favorable behavior during planing and molding operations, reflected in the production of uniform surfaces with low defect occurrence and adequate finishing quality. The joints and connections between components exhibited good dimensional accuracy, without significant deformations during the conditioning process. Likewise, the stability observed during drying and subsequent handling remained within acceptable ranges, with no visible warping or cracking, resulting in a final product with adequate structural integrity and homogeneous surface quality.

On the other hand, in the fabrication of desks, the wood showed consistent behavior during machining and assembly stages, particularly in planing and molding operations, where smooth and uniform surfaces were obtained. In drilling operations, slight internal irregularities were observed, consistent with the results of the drilling test; however, these did not compromise the final product quality and were corrected through finishing processes. During assembly, the components maintained adequate dimensional stability, allowing for proper fit in the joints and a functional structural configuration. Overall, the developed prototypes reflect the suitability of thinning wood of *Simarouba amara* Aubl. for use in secondary wood products, evidencing performance consistent with the experimentally obtained machinability results. The surface quality, processing stability, and structural integrity observed in both types of prototypes confirm the viability of the material for carpentry and furniture applications under controlled processing conditions.

Figure 12. Production process of prototypes from thinning wood of *Simarouba amara* Aubl. Prototypes manufactured in the Carpentry Workshop of CITEforestal Pucallpa, Technological Institute of Production (ITP). (**a**) Determination of the initial volume (m^3) of sawn wood. (**b**) Kiln drying of sawn wood in conventional drying chambers. The thicknesses processed were 1″, 1.5″, and 2″. (**c**) Assembly process of components for the fabrication of a wooden desk. (**d**) Pre-finishing process of a solid wood door. (**e**) Application of the first coat of varnish on wooden desks. (**f**) Final presentation of the desk prototype (130 cm × 60 cm × 75 cm) and solid wood door (205 cm × 83 cm), both finished using a sealed lacquer coating technique. The developed prototypes are currently exhibited at the Alexander von Humboldt Experimental Center, located in Padre Abad Province, Ucayali Region, Peru.

4. Discussion

The results obtained strengthen the hypothesis that planting density and the longitudinal position along the stem significantly influence the technological performance of *Simarouba amara* Aubl. thinning wood, as shown in Table 7.

Table 7. Physical properties of *Simarouba amara* Aubl. thinning wood under the influence of planting density and longitudinal stem position.

NLF	DS	CHSat	Cheh	PSF	TC	RC	LC	VC	BD	SD	AD	OD	DSI	VCC
Ba	2 × 2	96.17 (7.59) b	11.41 (0.73) f	26.80 (1.04) f	6.22 (0.63) f	3.77 (0.28) e	0.25 (0.04) f	10.18 (0.84) f	0.45 (0.03) ns	1.09 (0.06) ns	0.52 0.04 a	0.49 (0.03) ns	1.66 (0.21) ns	0.38 (0.03) ns
Me	2 × 2	109.09 (9.24) d	12.85 (0.86) d	29.94 (0.97) d	7.42 (0.80) d	4.25 (0.35) d	0.40 (0.06) d	12.05 (1.07) d	0.40 (0.03) ns	1.00 (0.06) ns	0.46 0.03 b	0.42 (0.03) ns	1.76 (0.25) ns	0.40 (0.04) ns
Ap	2 × 2	125.38 (9.86) e	14.58 (0.87) b	33.17 (1.02) b	8.82 (0.87) b	4.84 (0.35) b	0.65 (0.11) b	13.81 (1.14) b	0.34 (0.02) ns	0.92 (0.05) ns	0.40 0.03 d	0.36 (0.02) ns	1.83 (0.22) ns	0.42 (0.03) ns
Ba	3 × 3	106.94 (8.14) a	12.52 (0.66) e	29.15 (1.00) e	6.98 (0.58) e	4.21 (0.34) d	0.35 (0.05) e	11.55 (0.91) e	0.41 (0.02) ns	1.02 (0.06) ns	0.47 0.03 b	0.43 (0.03) ns	1.67 (0.18) ns	0.40 (0.04) ns
Me	3 × 3	122.06 (9.01) c	13.79 (0.83) c	31.97 (1.00) c	8.28 (0.82) c	4.58 (0.36) c	0.57 (0.08) c	13.27 (1.10) c	0.36 (0.03) ns	0.95 (0.05) ns	0.43 0.03 c	0.38 (0.02) ns	1.82 (0.24) ns	0.42 (0.04) ns
Ap	3 × 3	135.42 (9.93) d	15.54 (0.94) a	34.99 (1.03) a	9.41 (0.96) a	4.95 (0.43) a	0.85 (0.13) a	14.81 (1.14) a	0.30 (0.02) ns	0.88 (0.05) ns	0.36 0.03 e	0.32 (0.02) ns	1.91 (0.24) ns	0.42 (0.04) ns

Values without parentheses correspond to the mean values of each evaluated property, whereas values in parentheses represent the standard deviation. Different letters within the same column indicate statistically significant differences among treatments according to the multiple mean comparison test ($p < 0.05$); treatments sharing the same letter do not differ significantly. The abbreviation ns indicates the absence of statistically significant differences among the evaluated treatments ($p > 0.05$).

The observed variation in CHSat appears to be associated with differences in wood density and anatomical structure [41]. Lower density wood from the upper stem, particularly under the wider planting spacing, generally exhibits a greater proportion of void spaces and cell lumina, resulting in a higher water-holding capacity. Accordingly, CHSat values exceeding 130% in the apical portion of trees grown under the 3 × 3 m spacing are consistent with highly porous wood and high permeability. In contrast, wood sampled from the stem base exhibited lower CHSat values (96.17%), consistent with a lower capacity to retain free water, probably associated with lower porosity. Overall, these results suggest that longitudinal position within the stem had a greater influence on moisture saturation characteristics than planting spacing [42].

The PSF values (26.80%–34.99%) fall within the typical range reported for hardwood species (25%–35%) [43]. Their increase toward the apex and under wider spacing is attributed to the greater proportion of cell walls containing micropores [44] and the higher accessibility of hydroxyl (-OH) groups in juvenile wood [45]. Higher PSF values imply that wood begins to shrink at higher moisture contents during drying, which is critical for establishing appropriate drying schedules [46]. Therefore, for wood with high PSF values, lower initial drying temperatures and higher relative humidity levels in the drying chamber are recommended to prevent premature drying stresses [47]. For high-value products, slow drying is recommended for apex wood and wood grown at 3 × 3 m spacing to avoid collapse and checking. In contrast, base wood from the 2 × 2 m spacing treatment, with a lower PSF (26.8%), is more tolerant of rapid drying schedules. These findings are consistent with those reported by [48,49] regarding the relationship among basic density, fiber saturation point, and wood collapse.

The basic density of *S. amara* determined in this study (0.33–0.45 g cm^{-3}) classifies the wood as low to medium density, placing it close to *Ochroma pyramidale* (balsa) at the lighter end of the spectrum [50] and comparable to *Cedrela odorata* at the lower limit of the medium-density category [51]. The decrease in density from the base toward the apex (Figure 6) is consistent with the ontogenetic gradient. Wood at the base of the tree contains a greater proportion of mature wood, characterized by thicker fiber walls and smaller lumina, whereas wood formed toward the apex is predominantly juvenile, exhibiting thinner fiber walls, larger lumina, and consequently lower density [52]. This pattern has been widely reported by [53,54] for tropical species.

The effect of spacing on wood quality is significant; a narrower planting spacing (2 × 2 m) induces competitive stress that triggers adaptive mechanisms in the tree, such as the formation of reaction wood and the development of fibers with thicker cell walls to provide structural support, thereby increasing basic density [55,56]. In contrast, wider spacing (3 × 3 m) promotes more vigorous radial growth, although with a tendency toward a lower proportion of high-density wood [57]. In technological terms, wood density varied across a relatively low range overall, with basic density values ranging from 0.30 g cm^{-3} at the apex under 3 × 3 m spacing to 0.45 g cm^{-3} at the base under 2 × 2 m spacing (Figure 6). Although these variations across trunk positions and planting densities are moderate, air-dry density (AD) revealed significant differences among treatments. These results suggest that material from denser spacings of 2 × 2 m, particularly at the base, could be explored for light, non-structural carpentry or joinery [26]. Conversely, lower density material from apical sections under 3 × 3 m spacing is better suited for applications prioritizing low weight, such as core stock for light panels, packaging, or internal furniture components [6].

The results demonstrate a marked influence of longitudinal position and planting density on the shrinkage anisotropy of the material. The increase in dimensional instability from the base toward the apex is mainly attributed to differences in the physiological maturity of the tissue: in the basal section, more mature cellular elements predominate, with thicker cell walls and a denser xylem structure that restricts hygroscopic shrinkage [29]. In contrast, toward the apex, juvenile wood prevails, characterized by a higher microfibril angle in the S2 layer and a greater proportion of fibers with thin cell walls, factors that exacerbate deformation during the drying process [58]. This phenomenon is consistent with observations in various fast-growing tropical species, where the interaction between biological growth rate and spacing management defines stem homogeneity and technological quality [29,59].

Planting density (3 × 3 m) favors the development of more vigorous crowns and a higher production of juvenile wood, which explains the increase in shrinkage rates compared to the 2 × 2 m planting density, where early intraspecific competition generates tissues with higher basic density that act to reduce the magnitude of shrinkage [60,61]. The values recorded for the tangential-to-radial shrinkage ratio (TC/RC), ranging from 1.65 to 1.90, indicate wood with notable dimensional stability, a key factor for minimizing deformation risks and internal stresses during the drying process [29,62]. This stability is further reinforced by an exceptionally low longitudinal shrinkage (≤1.5%), which prevents critical defects such as axial warping and confirms the technological suitability of the material for the manufacture of high value-added products, such as fine furniture or precision components [63,64]. Finally, the combination of these physical properties with an excellent response to machining operations enables the efficient integration of *S. amara* thinning wood into high-demand secondary transformation processes [64].

The stability observed in the volumetric shrinkage coefficient (VCC) suggests that 13-year-old juvenile wood of *S. amara* exhibits a homogeneous hygroscopic response, an essential characteristic for predicting material behavior during drying and subsequent manufacturing processes [65,66]. The slight reduction in VCC observed at the base of trees under higher planting density (2 × 2 m) may be linked to growth stress dynamics and cellular differentiation that alter the ultrastructure of the cell wall, thereby mitigating deformation in that specific zone [67]. However, the numerical variation detected (0.38 vs. 0.41) is marginal in practical terms, confirming the uniformity of the resource for processing.

https://doi.org/10.3390/f17080915

Similar behaviors have been documented in other fast-growing species, where stability indices and shrinkage rates are more strongly governed by ontogenetic tissue maturity than by variations in initial planting density [51,68]. Consequently, the homogeneity of VCC across different stem positions allows this thinning wood to be classified as having predictable performance, facilitating its recognition and use as a quality commercial timber resource [24,59]. This technological consistency is essential for integrating the material into production lines that require superior surface finishing and high machining efficiency [64].

Regarding machinability, the results show a heterogeneous behavior conditioned by the nature of each machining operation. The excellent performance observed in planing and molding indicates an optimal response to longitudinal cutting, favored by the uniform texture and the low basic density (approximately 0.40) characteristic of *S. amara* [6,24]. This ease of processing is correlated with the species' moderate mechanical resistance, allowing for the production of high-quality surfaces with minimal defect incidence, which is essential for optimizing finishing processes in products such as furniture or musical instruments [6,69]. In contrast, the regular performance in the turning operation suggests limitations in transverse or rotational cutting processes, where surface quality critically depends on factors such as rake angle, feed rate, and anatomical structure [14,70]. This behavior is consistent with studies indicating that, in low-density and diffuse-porous woods, machining quality may be compromised by insufficient fiber cohesion during rotational cutting, requiring precise adjustment of machine parameters to avoid excessive roughness [71,72]. Finally, the possibility of improving these properties through thermo-mechanical treatments opens new opportunities for the use of this species in flooring or higher technical requirement components [73].

Validation through functional prototypes confirms that thinning wood of *S. amara* possesses remarkable industrial suitability, particularly in the execution of precision structural joints such as the mortise and tenon system, where fit accuracy is decisive for the mechanical strength and durability of furniture [74]. This ability to maintain stable fitting under service conditions is attributed to its favorable hygroscopic response, which minimizes the development of gaps or stresses at critical connection points under changes in environmental humidity [75,76]. Moreover, the surface quality and finishing achieved in commercially sized pieces demonstrate that processing wood from thinnings or secondary forests does not compromise either the esthetics or the technical functionality of the final product [77]. By integrating physical characterization with real performance testing, a utilization model is established that ensures both efficient raw material use and the structural integrity required for high value-added applications [78,79]. Consequently, this practical approach validates the transition from experimental analysis to industrial scale, ensuring consistent results in the machining and assembly of juvenile wood components [80].

From a broader perspective, the results contribute to the understanding of the valorization potential of thinning wood in tropical forest systems. Traditionally underutilized for low-value energy purposes such as firewood or charcoal [81,82], this raw material demonstrates suitable technical conditions for its incorporation into more complex value chains, including the manufacture of engineered wood products (such as CLT or LVL), textile fibers, and nanocellulose, aligning with circular bioeconomy approaches and the cascading use of biomass [83,84]. In this sense, the integration of technological criteria such as density and the management of juvenile wood proportion into silvicultural management allows thinning to be considered the "first transformation operation" of the product, optimizing wood characteristics for specific structural or industrial uses [26,85,86]. Moreover, the implementation of emerging technologies such as thermal modification offers a sustainable pathway to improve the stability and commercial competitiveness of thinning wood from fast-growing plantations [87].

https://doi.org/10.3390/f17080915

However, it is important to acknowledge certain limitations of this study. The evaluation focused on physical and machinability properties, omitting critical parameters of mechanical strength and natural durability against biological agents; this limitation restricts extrapolation to structural applications, where stress characterization and service life are essential regulatory requirements to ensure construction safety [81,87]. Likewise, the use of small samples under controlled laboratory conditions may not capture the technological variability present in thinning wood at an industrial scale, where factors such as knot presence and the higher proportion of juvenile wood in short rotations significantly alter material performance [26,86].

Accordingly, future research directions are proposed: (i) deeper mechanical characterization, given that preliminary studies on *S. amara* indicate that its resistance may reach strength class C20, enabling its use in small-scale structural applications and furniture [6,25]; (ii) evaluation of biological durability and response to thermomechanical treatments, which have been shown to significantly improve modulus of elasticity and esthetic quality for high-value niches such as flooring [73,88]; (iii) optimization of drying processes to take advantage of the low shrinkage and high dimensional stability exhibited by this species even at early plantation ages (20–25 years) [25,27]; and (iv) the use of anatomical microcharacterization (such as fiber wall thickness) as a rapid predictor of technological performance in underutilized Amazonian woods [89,90]. Furthermore, the implementation of predictive models and artificial intelligence algorithms applied to thinning management would allow for simulation of wood quality scenarios prior to harvest [91,92]. Overall, these results position *Simarouba amara* Aubl. thinning wood as a key component for the development of engineered products (glulam or OSB) that reduce dependence on overexploited species, alleviating pressure on natural forests and strengthening the regional bioeconomy [28,93].

The wood evaluated in this study originated from 13-year-old thinning operations and therefore represents predominantly juvenile material. Consequently, the technological properties reported here should be interpreted within the context of wood obtained from young plantations rather than mature stands. Nevertheless, the results demonstrate that *Simarouba amara* thinning wood possesses considerable potential for value-added applications, supporting the sustainable utilization of material generated during intermediate silvicultural treatments. Further evaluations of industrial processing performance, including sawing yield and recovery, are required to optimize the utilization of thinning wood and to better define its potential for commercial applications . Although anatomical characterization was beyond the scope of the present study, integrating wood anatomical analyses with technological property assessment could provide complementary information for a more comprehensive understanding of the relationships between wood structure and performance [90]. In addition, future studies comparing juvenile and mature wood harvested at different rotation ages would further elucidate the ontogenetic development of wood quality and provide a stronger scientific basis for optimizing both silvicultural management and industrial utilization of this species [94].

5. Conclusions

The results of this study suggest that planting density and longitudinal stem position significantly influence the physical, hygroscopic, and machinability properties of thinning wood of *Simarouba amara* Aubl., validating the proposed hypothesis and evidencing consistent patterns of axial and between-treatment variation. Moisture content and shrinkage increased progressively from the base toward the apex, with volumetric shrinkage values ranging from 10.18% to 14.81%, associated with a higher proportion of juvenile wood. Wood density generally showed higher mean values under the 2 × 2 m spacing, although statistically significant differences between planting spacings were only detected for air-dry density. Dimensional stability, evaluated through the T/R index (1.66–1.91) and the volumetric shrinkage coefficient (0.38–0.42), falls within moderate ranges, suitable for carpentry and furniture applications. Regarding machinability, the wood exhibited excellent performance in planing (VA = 1.18) and molding (VA = 1.02), good performance in drilling (VA = 1.88), and regular performance in turning (VA = 2.68), with the latter identified as the operation requiring optimization of processing parameters. Validation through functional prototypes confirms its suitability for secondary transformation products, showing coherence between experimental results and industrial performance. Overall, these findings suggest *Simarouba amara* Aubl. thinning wood as a viable resource for incorporation into higher value-added supply chains, contributing to the sustainability of the forestry sector. Future studies should address mechanical properties, durability, and the optimization of industrial processes to expand its field of application.

Supplementary Materials: The following supporting information can be downloaded at: https://www.mdpi.com/article/10.3390/f17080915/s1.

Author Contributions: Conceptualization, L.P.A.-C. and T.M.U.-A.; methodology, L.P.A.-C., T.M.U.-A., J.A.R.-S., H.F.-P., C.M.-M. and J.K.H.-B.; software, O.A.R.-T., W.F.G.-A., H.G.-A. and U.A.-P.; validation, J.A.R.-S., H.F.-P., C.M.-M., J.K.H.-B., O.A.R.-T., W.F.G.-A., H.G.-A., A.L.M.V.-V. and U.A.-P.; formal analysis, L.P.A.-C., T.M.U.-A., O.A.R.-T., W.F.G.-A., H.G.-A., A.L.M.V.-V. and U.A.-P.; investigation, L.P.A.-C.; resources, L.P.A.-C., R.M.B.-P. and K.I.R.-V.; data curation, O.A.R.-T., W.F.G.-A., H.G.-A., A.L.M.V.-V. and U.A.-P.; writing—original draft preparation, L.P.A.-C., R.M.B.-P., E.E.L.-G. and K.I.R.-V.; writing—review and editing, L.P.A.-C., R.M.B.-P., E.E.L.-G. and K.I.R.-V.; visualization, J.A.R.-S., H.F.-P., C.M.-M. and J.K.H.-B.; supervision, J.A.R.-S., H.F.-P., C.M.-M. and J.K.H.-B.; project administration, R.M.B.-P., E.E.L.-G. and K.I.R.-V.; funding acquisition, R.M.B.-P., E.E.L.-G. and K.I.R.-V. All authors have read and agreed to the published version of the manuscript.

Funding: This research received no external funding. The study received logistical support from the Pucallpa Agricultural Experimental Station and the CITEforestal Pucallpa of the Institute of Technological Production (ITP).

Data Availability Statement: The data supporting the findings of this study are available in the Supplementary Materials.

Acknowledgments: The authors acknowledge the National Institute of Agrarian Innovation (INIA), through the Pucallpa Agricultural Experimental Station, and the Institute of Technological Production (ITP), through the CITEforestal Pucallpa, for providing logistical and technical support, as well as institutional facilities for the development of this research. Likewise, the authors thank the researchers from the Universidad Nacional de Ucayali (UNU), the Universidad Nacional Toribio Rodríguez de Mendoza de Amazonas (UNTRM), and the Instituto de Investigaciones de la Amazonía Peruana (IIAP) for their collaboration and academic contributions. The authors also recognize the valuable participation of the technicians and assistants involved in fieldwork, as well as Walter Esteban Warshalowsky Navarro for his valuable support in conducting the laboratory measurements.

Conflicts of Interest: The authors declare that they have no conflicts of interest.

References

1. Wightman, K.E.; Cornelius, J.P.; Ugarte, L.J. El Raleo. In *¡Plantemos Madera! Manual Sobre el Establecimiento, Manejo y Aprovechamiento de Plantaciones Maderables Para Productores de la Amazonía Peruana*; World Agroforestry (ICRAF): Lima, Peru, 2006; p. 204, ISBN 92 9059 200 1. Available online: https://www.landscapealliance.org/knowledge/publication/33508/ (accessed on 4 May 2026).
2. Ronoud, G.; Poorazimy, M.; Yrttimaa, T.; Luoma, V.; Huuskonen, S.; Hynynen, J.; Hyyppä, J.; Saarinen, N.; Kankare, V.; Vastaranta, M. Terrestrial Laser Scanning in Assessing the Effect of Different Thinning Treatments on the Competition of Scots Pine (*Pinus sylvestris* L.) Forests. *Remote Sens.* **2022**, *14*, 5196. [CrossRef]

3. Espinosa, M.; Muñoz, F. Raleo En Bosques Plantados. In *Silvicultura de Bosques Plantados con Fines Productivos*; Sello Editorial Monografias: Concepcion, Chile, 2017; Volume 1, pp. 179–216, ISBN 978-956-227-416-6. Available online: https://forestal2.udec.cl/investigacion/libros/ (accessed on 29 July 2026).
4. Díaz Bravo, S.; Espinosa, M.; Valenzuela, L.; Cancino, J.; Lasserre, J.P. Efecto Del Raleo En El Crecimiento y Algunas Propiedades de La Madera de Eucalyptus Nitens En Una Plantación de 15 Años. *Maderas Cienc. Tecnol.* **2012**, *14*, 373–388. [CrossRef]
5. Gagnon, B.; Tanguay, X.; Amor, B.; Imbrogno, A.F. Forest Products and Circular Economy Strategies: A Canadian Perspective. *Energies* **2022**, *15*, 673. [CrossRef]
6. Martins, M.; Bufalino, L.; Gouvea, L. Wood Characterization of Marupá (*Simarouba amara* Aubl, Simaroubaceae) for Use in the Furniture Industry. *Braz. J. Dev.* **2020**, *6*, 98163–98185. [CrossRef]
7. Alegre, J.; Lao, C.; Silva, C.; Schrevens, E. Recovering Degraded Lands in the Peruvian Amazon by Cover Crops and Sustainable Agroforestry Systems. *Peruv. J. Agron.* **2017**, *1*, 1–7. [CrossRef]
8. Soudre, M.; Vidal, F.; Mori, J.; Guerra, H.; Mesen, F.; Perez, F. Propagación Vegetativa de Marupa (*Simarouba amara* Aubl.) Medinte Eraizamiento de Estacas Juveniles En Propagador de Subirrigación. *Folia Amaz.* **2010**, *19*, 61–68. Available online: http://www.iiap.org.pe/Archivos/Publicaciones/PUBL808.pdf (accessed on 20 May 2026). [CrossRef]
9. Ugarte, J.; Roman, F. Tasas de Crecimiento de Cuatro Especies Nativas En Plantaciones Forestales Comerciales En Cuatro Regiones de La Amazonía Peruana. *Rev. For. Perú* **2020**, *35*, 44. [CrossRef]
10. ONF. *Ingenieria de La Madera*; Oficina Nacional Forestal: San Jose, Costa Rica, 2015.
11. Fuentes, F.J.; Silva, J.A.; Rodríguez, R.; Sanjuán, R.; Richter, H. Perfil De Estabilidad Dimensional De Las Maderas Primavera Y Rosa Morada. *Rev. Mex. Cienc. For.* **2018**, *5*, 56–69. [CrossRef]
12. Liao, Z.; Schoop, J.M.; Saelzer, J.; Bergmann, B.; Priarone, P.C.; Splettstoßer, A.; Bedekar, V.; Zanger, F.; Kaynak, Y. Review of Current Best-Practices in Machinability Evaluation and Understanding for Improving Machining Performance. *CIRP J. Manuf. Sci. Technol.* **2024**, *50*, 151–184. [CrossRef]
13. Emmerich, L.; Wülfing, G.; Brischke, C. The Impact of Anatomical Characteristics on the Structural Integrity of Wood. *Forests* **2019**, *10*, 199. [CrossRef]
14. de Almeida, A.; Rodrigues, T.; Moreira, J.; Costa, S.; Cardozo, A.; Tarcísio, J. Influence of Basic Wood Density on the Specific Cutting Energy. *Res. Soc. Dev.* **2022**, *11*, 1–10. [CrossRef]
15. Hanincová, L.; Procházka, J.; Novák, V.; Kopecký, Z. Influence of Moisture Content on Cutting Parameters and Fracture Characteristics of Spruce and Oak Wood. *Drv. Indistrija* **2022**, *73*, 341–349. [CrossRef]
16. Gonçalves, R.; Néri, A. Orthogonal cutting forces in juvenile and mature pinus taeda wood. *Sci. Agric.* **2005**, *62*, 310–318. [CrossRef]
17. Korkmaz, M.; Budakçı, M.; Kılınç, İ. Assessment of Surface Roughness in Milling of Wood with Different Material Temperature and Cutting Parameters. *Bioresources* **2024**, *19*, 9343–9357. [CrossRef]
18. Oliveira, T.; Moreira, J.; Gherardi, P.; Costa, S. Cutting Energy Required during the Mechanical Processing of Wood Species at Different Drying Stages. *Maderas Cienc. Tecnol.* **2020**, *22*, 477–482. [CrossRef]
19. *ASTM D1666-22*; Standard Test Methods for Conducting Machining Tests of Wood and Wood-Base Panel Materials. Advancing Standards Transforming Markets; ASTM International: West Conshohocken, PA, USA, 2022; Volume 04.10.
20. Martínez-Pinillos, E.; Martinez, J.L. Características de Cepillado y Lijado de 33 Especies de Madera. *Madera Bosques* **2016**, *2*, 11–27. [CrossRef]
21. Roussel, J.R.; Clair, B. Evidence of the Late Lignification of the G-Layer in Simarouba Tension Wood, to Assist Understanding How Non-G-Layer Species Produce Tensile Stress. *Tree Physiol.* **2015**, *35*, 1366–1377. [CrossRef] [PubMed]
22. Ryan, M.G.; Hubbard, R.M.; Clark, D.A.; Sanford, R.L. Woody-Tissue Respiration for *Simarouba amara* and *Minquartia guianensis*, Two Tropical Wet Forest Trees with Different Growth Habits. *Oecologia* **1994**, *100*, 213–220. [CrossRef] [PubMed]
23. Elvas Costa, J.E.; do Nascimento, C.C.; de Araújo, R.D.; Pacheco, K.M.M. Evaluation of the Quality of Wood from Naturally Fallen Tree for the Development of Products in Design. *Int. J. Innov. Educ. Res.* **2021**, *9*, 172–187. [CrossRef]
24. Hoffmann, W.R.; Campos, C.M.; Stragliotto, M.C.; Oliveira, A.C.; Pereira, B.L.C. Macroscopic Anatomy as a Strategy for Recognizing Commercial Wood from the Brazilian Amazon. *Bioresources* **2025**, *20*, 10300–10327. [CrossRef]
25. Quintana, S.; Cabudivo, A.; Espiritu, J.M.; Cabudivo, J.M. Propiedades Físico-Mecánicas de Las Maderas de *Simarouba amara* (Aubl.) y Cedrelinga Cateniformis (Ducke) de Plantaciones de Diferentes Edades, San Juan Bautista, Loreto, Peru. *Conoc. Amaz.* **2011**, *2*, 115–123. Available online: https://revistas.unapiquitos.edu.pe/index.php/Conocimientoamazonico/article/view/36 (accessed on 20 May 2026).
26. Barrette, J.; Achim, A.; Auty, D. Impact of Intensive Forest Management Practices on Wood Quality from Conifers: Literature Review and Reflection on Future Challenges. *Curr. For. Rep.* **2023**, *9*, 101–130. [CrossRef]
27. Seta, G.W.; Hidayati, F.; Widiyatno; Na'iem, M. Wood Physical and Mechanical Properties of Clonal Teak (Tectona Grandis) Stands under Different Thinning and Pruning Intensity Levels Planted in Java, Indonesia. *J. Korean Wood Sci. Technol.* **2023**, *51*, 109–132. [CrossRef]

28. Fauziyyah, S.; Wimmer, R.; Halmschlager, E.; Brischke, C. Unlocking the Potential of Fast-Growing Species from Indonesia: Durability and Sorption Aspects. *Bois For. Trop.* **2023**, *358*, 39–52. [CrossRef]
29. Tenorio, C.; Moya, R.; Salas, C.; Berrocal, A. Evaluation of Wood Properties from Six Native Species of Forest Plantations in Costa Rica. *Bosque* **2016**, *37*, 71–84. [CrossRef]
30. INIA. *Parámetros Edaficos de Las Parcelas Muestreadas*; INIA: Pucallpa, Peru, 2026.
31. *NTP 251.008*; Madera y Carpinteria Para Construccion. Seleccion y Coleccion de Muestras. Direccion de Normalizacion—INACAL: Lima, Peru, 2023.
32. *ISO 4471-1982*; Madera—Muestreo de Árboles y Trozas Para La Determinación de Las Propiedades Físicas y Mecánicas de La Madera En Rodales Homogéneos. ISO: Geneva, Switzerland, 1982.
33. *NTP 251.009*; Madera y Carpinteria Para Construcción. Acondicionamiento de Las Maderas Destinada a Ensayos Fisicos y Mecanicos. Direccion de Normalizacion—INACAL: Lima, Peru, 2016.
34. *NTP 251.011*; Madera. Metodo Para Determinar La Densidad. Direccion de Normalizacion—INACAL: Lima, Peru, 2019.
35. *ASTM D5536-17*; Standard Practice for Sampling Forest Trees for Determination of Clear Wood Properties. Advancing Standards Transforming Markets; ASTM International: West Conshohocken, PA, USA, 2023; Volume 04.10.
36. Rodriguez, J.; Maguiña, F.; Apuela, A.; Rodriguez, K. *Determinación de La Trabajabilidad de La Especie* Simarouba Amara *Aubl., Procedente de Raleo de Una Plantación de Trece Años En La Region Ucayali*; Informe Técnico de Servicio, CITEforestal Pucallpa del Instituto Tecnologico de la Produccion: Pucallpa, Peru, 2025.
37. JUNAC. *Manual de Diseño Para Maderas Del Grupo Andino*, Tercera ed.; Carmona, P., Moncayo, E., Camacho, E., Eds.; Proyectos Andinos de Desarrollo Tecnologico en el Area de los Recursos Forestales Tropicales de la Junta del Acuerdo de Cartagena: Lima, Peru, 1984.
38. *NTP 251.010*; Madera. Metodo Para Determinar El Contenido de Humedad. Direccion de Normalizacion—INACAL: Lima, Peru, 2014.
39. *NTP 251.012*; Madera. Metodo Para Determinar La Contraccion. Direccion de Normalizacion—INACAL: Lima, Peru, 2015.
40. Guadalupe Baylon, N.K.; Diaz Zuñiga, E.J.; Ruiz Morales, J. *Meteorología UNU*; Universidad Nacional de Ucayali (UNU): Pucallpa, Peru, 2024.
41. Duruaku, J.I.; Okoye, P.A.C.; Okoye, N.H.; Nwadiogbu, J.O.; Onwukeme, V.I.; Arinze, R.U. An Evaluation of the Physicochemical, Structural and Morphological Properties of Selected Tropical Wood Species for Possible Utilization in the Wood Industry. *J. Sustain. Bioenergy Syst.* **2023**, *13*, 131–148. [CrossRef]
42. Benitez, F.M.; de Nazaré Oliveira Novais, T.; Gonçalves, L.A.; Braga, E.; Barbosa de Castro, R.; Sousa, J.; Flores, E.; Fearnside, P.M. Wood Basic Density in Large Trees: Impacts on Biomass Estimates in the Southwestern Brazilian Amazon. *Forests* **2024**, *15*, 734. [CrossRef]
43. Berry, S.L.; Roderick, M.L. Plant-Water Relations and the Fibre Saturation Point. *New Phytol.* **2005**, *168*, 25–37. [CrossRef] [PubMed]
44. Zauer, M.; Kretzschmar, J.; Großmann, L.; Pfriem, A.; Wagenführ, A. Analysis of the Pore-Size Distribution and Fiber Saturation Point of Native and Thermally Modified Wood Using Differential Scanning Calorimetry. *Wood Sci. Technol.* **2014**, *48*, 177–193. [CrossRef]
45. Fredriksson, M.; Rüggeberg, M.; Nord-Larsen, T.; Beck, G.; Thybring, E.E. Water Sorption in Wood Cell Walls–Data Exploration of the Influential Physicochemical Characteristics. *Cellulose* **2023**, *30*, 1857–1871. [CrossRef]
46. Hernández, R.E.; Pontin, M. Shrinkage of Three Tropical Hardwoods below and above the Fiber Saturation Point. *Wood Fiber Sci.* **2006**, *38*, 474–483. Available online: https://wfs.swst.org/index.php/wfs/article/view/1233 (accessed on 20 May 2026).
47. Majka, J.; Sydor, M. Analysis of Stress Development during Kiln Drying of Beech Timber. *Eur. J. Wood Wood Prod.* **2023**, *81*, 1189–1200. [CrossRef]
48. Chafe, S.C. Preheating and Continuous and Intermittent Drying in Boards of *Eucalyptus regnans* F. Muell. *Holzforschung* **1995**, *49*, 227–233. [CrossRef]
49. Pereira, P. Avaliação e Modelagem de Colapso Em Madeiras de Eucalyptus Grandis. Título de Mestre, Universidad Federal de Lavras. 2018. Available online: https://repositorio.ufla.br/server/api/core/bitstreams/4786ff43-17c8-46dd-a39b-070dc (accessed on 20 May 2026).
50. Jang, E.S.; Kang, C.W. Porosity Analysis of Three Types of Balsa (*Ochroma pyramidale*) Wood Depending on Density. *J. Wood Sci.* **2022**, *68*, 10–15. [CrossRef]
51. Honorato, J.A.; Sanches, V.; Perez, J. Variability of Some Wood Physical Properties of Ten *Cedrela odoratoa* L. Clones. *J. Agric. Sci. Res.* **2023**, *3*, 1–7. [CrossRef]
52. Martínez, H.I.; Jones, C.S.; Espino, S.; Schenk, H.J. Wood Anatomy and Wood Density in Shrubs: Responses to Varying Aridity along Transcontinental Transects. *Am. J. Bot.* **2009**, *96*, 1388–1398. [CrossRef] [PubMed]
53. Larson, P.R. *Wood Formation and the Concept of Wood Quality*; Yale University, School of Forestry: New Haven, CT, USA, 1969. Available online: https://research.fs.usda.gov/treesearch/49814 (accessed on 8 June 2026).

54. de Oliveira, A.; Farinassi, R.; Marin, L.; Akira, F.; de Souza, R.Q. Shrinkage of the Toona Ciliata Wood from Three Counties in the South of Minas Gerais State. *Cerne* **2014**, *20*, 351–361. [CrossRef]
55. de Lima, L.E.; Silva, C.d.J.; de Paula, T.; da Silva, G.; Souza, I.; Urbinati, C.V.; Trugilho, P.F.; Mori, F.A. Planting Density Effect on Some Properties of *Schizolobium parahyba* Wood. *Maderas Cienc. Tecnol.* **2018**, *20*, 381–394. [CrossRef]
56. Gril, J.; Jullien, D.; Bardet, S.; Yamamoto, H. Tree Growth Stress and Related Problems. *J. Wood Sci.* **2017**, *63*, 411–432. [CrossRef]
57. Hanumanthappa, D.C.; Bhaskar, V.; Ganesha, B.H.; Kumar, R. Performance of Melia Dubia under Different Planting Densities: Effects on Growth and Carbon Sequestration. *Curr. Sci.* **2025**, *129*, 169–174. [CrossRef]
58. Pérez, D. Stand Growth Scenarios for Tectona Grandis Plantations in Costa Rica. Available online: https://www.dissertationesforestales.fi/article/1784 (accessed on 20 May 2026).
59. Leroy, M.; Candelier, K.; Damay, J.; Bossu, J.; Thevenon, M.; Beauchene, J.; Clair, B.; Leroy, M.; Candelier, K.; Damay, J.; et al. Natural Durability of 8 Tropical Species Suitable for Round Wood Building: Fungal and Termites Laboratory Screening Tests. *Bois For. Trop.* **2024**, *1*, 1–39.
60. Zhang, S.Y.; Ren, H.; Jiang, Z. Wood Density and Wood Shrinkage in Relation to Initial Spacing and Tree Growth in Black Spruce (*Picea mariana*). *J. Wood Sci.* **2021**, *67*, 1–10. [CrossRef]
61. Ahmad, M.H.; Amini, M.M.; Sobri, S.A.; Sakagami, H.; Hermawan, A. Effect of Radial Growth Rate on Wood Properties Variation of Sentang (*Azadirachta excelsa*) Tree Planted in Kelantan, Malaysia. *Bioresources* **2023**, *18*, 5013–5027. [CrossRef]
62. Van Duong, D.; Matsumura, J. Transverse Shrinkage Variations within Tree Stems of Melia Azedarach Planted in Northern Vietnam. *J. Wood Sci.* **2018**, *64*, 720–729. [CrossRef]
63. Narh, J.L.; Appiah-Kubi, E.; Dadzie, P.K. Machining Qualities of Sapwood and Heartwood of Two Lesser Utilized Timber Species. *J. Hortic. For.* **2025**, *17*, 29–37. [CrossRef]
64. de Paula, M.H.; Silva, R.R.; de Almeida, M.; Gonçalez, J.C.; Ananías, R.A.; Janin, G. Effect of Applying Finishing Products and Sanding on the Surface of Marupa Wood. *Maderas Cienc. Tecnol.* **2020**, *22*, 45–54. [CrossRef]
65. De Carvalho, S.R.; Sousa, J.; da Silveira, N. Analysis of the Physical Properties of Mahogany (*Swietenia macrophylla* King) Wood in a Planted Forest in Central Amazonia. *Braz. J. Anim. Environ. Res.* **2021**, *4*, 2749–2763. [CrossRef]
66. Serenini, L.; de Melo, R.R.; Stangerlin, D.M.; Pimenta, A.S. Wood Quality of Six Eucalyptus Clones Planted in Northern Mato Grosso State, Brazil. *Wood Res.* **2020**, *65*, 543–554. [CrossRef]
67. Thibaut, B.; Gril, J. Tree Growth Forces and Wood Properties. *Peer Community J.* **2021**, *1*, 1–31. [CrossRef]
68. Kord, B.; Kialashaki, A.; Kord, B. The Within-Tree Variation in Wood Density and Shrinkage, and Their Relationship in Populus Euramericana. *Turk. J. Agric. For.* **2010**, *34*, 121–126. [CrossRef]
69. Goncalves, M.d.S. Trabalhabilidade Da Madeira Com Testes de Plaina, Lixa, Furacão e Torno Em Seis Espécies Madeireiras Da Regiao Amazônica. Monografia para obtencao de grau de Tecnologa Florestal, Instituto de Tecnologia da Amazonia—UTAM. 1990. Available online: https://www.alice.cnptia.embrapa.br/alice/handle/doc/666961?locale=en (accessed on 12 June 2026).
70. Cristóvão, L.; Broman, O.; Grönlund, A.; Ekevad, M.; Sitoe, R. Main Cutting Force Models for Two Species of Tropical Wood. *Wood Mater. Sci. Eng.* **2012**, *7*, 143–149. [CrossRef]
71. Eyma, F.; Méausoone, P.J.; Martin, P. Study of the Properties of Thirteen Tropical Wood Species to Improve the Prediction of Cutting Forces in Mode B. *Ann. For. Sci.* **2004**, *61*, 55–64. [CrossRef]
72. Loc, N.H.; Hung, T.Q. Optimization of Cutting Parameters on Surface Roughness and Productivity When Milling Wood Materials. *J. Mach. Eng.* **2021**, *21*, 72–89. [CrossRef]
73. Salgado, A.; Gonçalez, J.C.; Del Menezzi, C.H. Tratamento Termomecânico e Seus Efeitos Nas Propriedades Da *Simarouba amara* (Aubl.). *Floresta E Ambiente* **2016**, *23*, 565–572. [CrossRef]
74. Elek, L.; Kovács, Z.; Csóka, L.; Agarwal, C. Evaluation of the Effect of Optimal Fit Criteria on the Compressive Strength of Open Mortise and Tenon Corner Joints. *Eur. J. Wood Wood Prod.* **2020**, *78*, 351–363. [CrossRef]
75. Belleville, B. Improving Quality of Wood Products. Specification on Joining Methods for Various Types of Components and Products to Maximise Wood Recovery and Strength of Products. 2015. Available online: https://hdl.handle.net/11343/91072 (accessed on 20 May 2026).
76. Salzberger, M.; Rojas, J.S.C.; Koskamp, G. Moisture-Induced Timber Joining—Utilizing the Hygroscopicity and Shape-Memory Effect of Wood Resulting in Dimensional Change in a Prefabricated Wood-Only, Self-Built, Sawn Timber System for Affordable Housing in Colombia. *Res. Sq.* **2024**, 1–46, *Preprint*. [CrossRef] [PubMed]
77. Meléndez, M.; Juízo, C.G.F.; Bustamante, N.; Gonzáles, H.E.; Klitzke, R.J.; Pereira, M. Surface Quality of Peruvian Amazon Woods Submitted for Planning and Sanding. *Floresta* **2019**, *49*, 671–680. [CrossRef]
78. Djamhuri, N.S.; Oka, G.M.; Chauf, K.A. Analysis of Two-Side Wood Joints Using the European Yield Model (EYM) Method Referring to SNI 7973:2013. *Int. J. Innov. Sci. Res. Technol.* **2025**, *10*, 1718. [CrossRef]
79. Iru, R.; Belleville, B.; Tsiritsi, C.; Ozarska, B. Enhancing the Knowledge of Wood Properties and Processing Characteristics of PNG Timbers. Machining Characteristics of PNG Timber Species. 2019. Available online: https://hdl.handle.net/11343/220473 (accessed on 20 May 2026).

80. Vieira, J.; Manzoni, F.; Brixner, J.B.; Baldissera, L.P.; Cuchi, T.; Schlickmann, M.B. Technological Characterization of Mezilaurus Itauba Wood: Application and Machining Tests. *Floresta* **2021**, *51*, 37–43. [CrossRef]
81. Bukauskas, A.; Mayencourt, P.; Shepherd, P.; Sharma, B.; Mueller, C.; Walker, P.; Bregulla, J. Whole Timber Construction: A State of the Art Review. *Constr. Build. Mater.* **2019**, *213*, 748–769. [CrossRef]
82. Lu, H. Towards Sustainability: An Optimization Framework for the Australian Hardwood Plantation Mid-Thinning Management Using Life Cycle Approach. Ph.D. Thesis, Griffith University, Nathan, Australia, 2017. [CrossRef] [PubMed]
83. Ali, A.; Russell, J.D. Accelerating the Transition to Wood-Based Circular Bioeconomy: A Literature Review of Current State, Trends, Opportunities, and Priorities for Future Research. *Curr. For. Rep.* **2025**, *11*, 1–20. [CrossRef]
84. Imparato, Y.; Hassegawa, M.; Verkerk, P.J.; Missio, A.L. Forest Bioeconomy in Brazil: Potential Innovative Products from the Forest Sector. *Land* **2022**, *11*, 1297. [CrossRef]
85. Vignote, S.; Martinez, I.; Villasante, A. La Silvicultura Como Primera Operacion de Transformacion de La Madera. *Rev. Mex. Cienc. For.* **2019**, *2*, 1–8. [CrossRef]
86. Resquin, F.; Baez, K.; de Freitas, S.; Passarella, D.; Coelho, A.P.; Rachid, C. Impact of Thinning on the Yield and Quality of Eucalyptus Grandis Wood at Harvest Time in Uruguay. *Forests* **2024**, *15*, 810. [CrossRef]
87. Wentzel, M.; Sepulveda, V.; Barros, J.L.; Ananias, R.A.; Rolleri, A. Chemical Structural Characteristics and Some Mechanical and Physical Properties of Thermally Modified Nothofagus Alpina Thinning Wood from Three Different Silvicultural Conditions. *Bioresources* **2024**, *19*, 6009–6024. [CrossRef]
88. Méndez, L.D.; Moya, R. Effect of Thermo-Treatment on the Physical and Mechanical, Color, Fungal Durability of Wood of Tectona Grandis and Gmelina Arborea from Forest Plantations. *Medziagotyra* **2018**, *24*, 59–68. [CrossRef]
89. Melo, G.; Silva, T.; dos Santos, L.D.J.; Oliveira, D.Y.; Vieira, L.; Braga Júnior, M.M.; Lopes, R.S.; Carvalho, F.W.; Macedo, A.L.; Costa, A.; et al. Anatomical Predictors of Density and Hardness in Underutilized Amazonian Woods: A Basis for Substituting Commercial Timbers. *For. Prod. J.* **2026**, *76*, 48–70. [CrossRef]
90. Fossi, C.G.; Christoforo, A.L.; Rocco, F.A. Correlations among Select Properties and Anatomical Parameters of Dipteryx Odorata Wood. *Rev. Mater.* **2025**, *30*, 1–9. [CrossRef]
91. Blanco, J.A.; Lo, Y.H. Latest Trends in Modelling Forest Ecosystems: New Approaches or Just New Methods? *Curr. For. Rep.* **2023**, *9*, 219–229. [CrossRef]
92. Pretzsch, H.; Poschenrieder, W.; Uhl, E.; Brazaitis, G.; Makrickiene, E.; Calama, R. Silvicultural Prescriptions for Mixed-Species Forest Stands. A European Review and Perspective. *Eur. J. For. Res.* **2021**, *140*, 1267–1294. [CrossRef]
93. Mishra, A.; Humpenöder, F.; Churkina, G.; Reyer, C.P.O.; Beier, F.; Bodirsky, B.L.; Schellnhuber, H.J.; Lotze-Campen, H.; Popp, A. Land Use Change and Carbon Emissions of a Transformation to Timber Cities. *Nat. Commun.* **2022**, *13*, 1–12. [CrossRef] [PubMed]
94. Troncones, A.G.; Gurau, L.; Porojan, M.; Stanciu, M.D. Identification of the Juvenile Wood Transition Age and of Some Growth Characteristics in Plantation vs. Native Populations of Cuban Pinus Caribaea M. Var. Caribaea B&G. *Bioresources* **2025**, *20*, 6242–6266. [CrossRef]